energies

MDPI

Review

A Review of Modular Electrical Sub-Systems of Electric Vehicles

Ahmed Darwish [1,2], Mohamed A. Elgenedy [3,*] and Barry W. Williams [4]

[1] School of Engineering, Faculty of Engineering and Digital Technologies, University of Bradford, Bradford BD7 1AZ, UK; a.badawy4@bradford.ac.uk or a.badawy@lancaster.ac.uk
[2] School of Engineering, Lancaster University, Lancaster LA1 4YR, UK
[3] School of Computing, Engineering and the Built Environment (SCEBE), Glasgow Caledonian University, Glasgow G4 0BA, UK
[4] Electronic and Electrical Engineering Department, Strathclyde University, Glasgow G1 1XQ, UK; barry.williams@strath.ac.uk
* Correspondence: mohamed.elgenedy@gcu.ac.uk

Abstract: Climate change risks have triggered the international community to find efficient solutions to reduce greenhouse gas (GHG) emissions mainly produced by the energy, industrial, and transportation sectors. The problem can be significantly tackled by promoting electric vehicles (EVs) to be the dominant technology in the transportation sector. Accordingly, there is a pressing need to increase the scale of EV penetration, which requires simplifying the manufacturing process, increasing the training level of maintenance personnel, securing the necessary supply chains, and, importantly, developing the charging infrastructure. A new modular trend in EV manufacturing is being explored and tested by several large automotive companies, mainly in the USA, the European Union, and China. This modular manufacturing platform paves the way for standardised manufacturing and assembly of EVs when standard scalable units are used to build EVs at different power scales, ranging from small light-duty vehicles to large electric buses and trucks. In this context, modularising EV electric systems needs to be considered to prepare for the next EV generation. This paper reviews the main modular topologies presented in the literature in the context of EV systems. This paper summarises the most promising topologies in terms of modularised battery connections, propulsion systems focusing on inverters and rectifiers, modular cascaded EV machines, and modular charging systems.

Keywords: electric vehicles (EVs); on-board battery chargers (OBCs); power factor correction (PFC); auxiliary power module (APM); propulsion system; traction inverter

Citation: Darwish, A.; Elgenedy, M.A.; Williams, B.W. A Review of Modular Electrical Sub-Systems of Electric Vehicles. *Energies* **2024**, *17*, 3474. https://doi.org/10.3390/en17143474

Academic Editor: Atriya Biswas

Received: 9 June 2024
Revised: 8 July 2024
Accepted: 10 July 2024
Published: 15 July 2024

1. Introduction

The persistent international desire to reduce harmful emissions resulting from the energy production process promotes electric vehicles (EV) over conventional internal combustion engine (IEC) vehicles in the transportation sector [1,2]. It is reported that more than two-thirds of the petroleum consumption is attributable to the transportation sector [3]. Accordingly, several countries are determined to reduce their dependencies on fossil fuel-based vehicles to comply with the Paris Climate Agreement clauses. In 2020, the China Association of Automobile Manufacturers (CAAM) reported that more than 1.2 million EVs were manufactured and sold [4]. In California, USA, there is an ambitious goal to end IEC vehicle production and sales by 2035 [5]. To meet this objective, the USA government has announced a massive investment to increase electric light-duty vehicle sales from 7.83% in 2023 to 100% in 2035–2040 [5]. European countries such as Germany, France, and the United Kingdom are establishing similar investments to win this transportation sector race.

The main electrical components of a typical 100% battery EV (BEV) are shown in Figure 1 including a high-voltage (HV) battery, electric motor, traction inverter, onboard charger (OBC), and low-voltage (LV) battery [6]. The HV battery system is usually fitted into the lower chassis of a vehicle to use the largest available planar space. In the present

common EV structures, the value of the battery's total voltage varies between 400 V and 800 V according to the number of series/parallel connected battery cells. Increasing the voltage of the HV system by adding more battery cells in series can add advantages to the EV system such as reducing the tractive system's current, reducing the size of the power cables, and increasing the operational speed of the motor, which reduces the gearbox/differential weight and size [7]. However, increasing the operational voltage above 800 V can create significant hazards to the electrical system as well as customers and maintenance personnel [8]. Also, the charging and balancing operation by the battery management system (BMS) becomes more complicated as the HV system's voltage increases. There is still debate about the optimum value of the tractive system's voltage, which determines the battery system's construction [7].

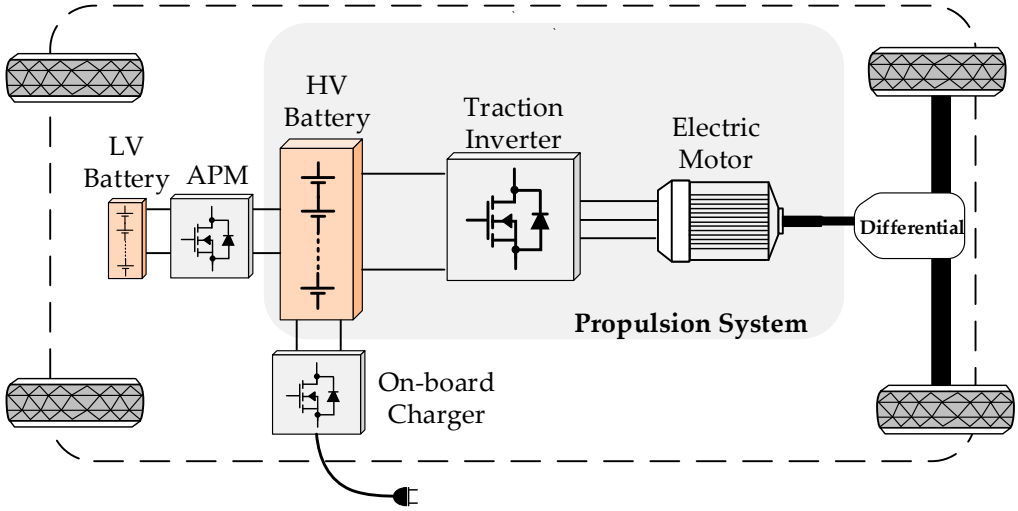

Figure 1. EV charging system with on-board and off-board chargers.

The electrical (machines) motors are responsible for producing the necessary torque, and, hence, force, to change the speed of the EV. Four main types of electric motors have been used in the context of EVs [9] including the following:

i. The permanent magnet brushed DC (PMBDC) motor was employed in earlier EVs because of its simple construction and control [2]. The PMBDC operates at DC voltages and currents and, therefore, a simple chopper circuit can be used at the control stage.

ii. Unlike the PMBDC, the induction motor (IM) does not have carbon brushes and, therefore, is preferred for robustness and reliability [10]. Additionally, because of its simple control, several Tesla EV models employ IMs with a conventional voltage source inverter (VSI) as the traction inverter [9]. More complex control techniques, such as field-oriented control (FOC), maximise the motor's torque and reduce the total harmonic distortion (THD) of the VSI's voltages and currents [10]. The IM is preferred for its high torque-to-mass ratio to reduce EV weight, an important factor in determining efficiency, by reducing the required energy absorbed from the battery.

iii. The permanent magnet synchronous motor (PMSM) is also employed in the EV industry because of its high torque and power [11]. The main difference between the PMSM and the IM is that the former's rotor is manufactured using a permanent magnet material that does not need excitation. The PMSM can be controlled by a traction inverter, such as a VSI, to operate with sinusoidal voltages and currents in the three phases. In this case, the motor output torque is constant with time, which improves EV performance and smooths speed. The PMSM can also be controlled by the traction inverter to push–pull the magnetic rotor according to its initial position and, hence, the voltages and currents in the phases pulsate [12]. In this mode, the

PMSM operates as a brushless DC (BLDC) motor, which is used extensively in the EV industry because it provides simple control without sacrificing efficiency [13]. One drawback of a PMSM-based propulsion system is that the rotor's position needs to be measured continuously during operation using sensors, which adds to system cost and complexity [14].

iv. The switched reluctance motor (SRM) is drawing increased attention in the field of EVs because its rotor can be manufactured using a soft iron material [15]. This reduces the weight and cost of the propulsion system, with no dependency on magnetic materials. SRM suffer from a high ripple torque, which in turn affects the EV speed profile and increases acoustic noise and vibration [16]. Also, SRM efficiency is lower than its IM and PMSM counterparts [17]. SRM variations are the synchronous SRM, with added PMs. Table 1 summarises the features of each motor type.

Table 1. Comparison of EV traction machines.

Motor	Advantages	Disadvantages	Example
DC	■ Torque–speed curve is suitable for EV traction. ■ Simple speed control typically with an H-bridge motor controller.	■ Bulky construction and low efficiency (≈85%). ■ Low reliability and high maintenance due to commutating brushes. ■ Relatively low power in EV applications because of space and drive. ■ Relatively old EV technology. ■ Low speed (<4000 rpm).	■ Model: 2005 Citroën Berlingo électrique. Technology: Separately exciter. Max. Power: 15.5 kW. Voltage: 400 V dc. Peak torque: 180 Nm. Max. Speed: 1600 rpm.
IM	■ High reliability and low maintenance. ■ Light because of the absence of magnetic materials. ■ Higher efficiency than DC motors (>92%). ■ High critical speed. ■ Low cost. ■ High power-to-weight ratio.	■ Efficiency deteriorates at high speeds, beyond critical speed because of rotor copper losses. ■ Power factor lower than PMSM. ■ Control is more complex than PMBDC motors.	■ Model: 2012–present Tesla Model S. Technology: 3-phase AC squirrel cage. Max. Power: 300 kW. Voltage: 400 V. Peak torque: 650 Nm. Max. Speed: 6000 rpm.
PMSM	■ The most common motor technology in the EV sector. ■ High effeiciency at all speeds, which can exceed 95%. ■ Good power-to-weigh ratio. ■ High power factor. ■ Excellent torque control.	■ Expensive because of the cost of the rotor's magnetic material. ■ Risk of rotor demagnitisation at very high speeds. ■ Complex control in comparison with PMBDC motors. ■ Depends on magnetic materials that are subject to supply chain issues.	■ Model: 2017–present Tesla Model 3. Technology: PMSM. Max. Power: 208 kW. Voltage: 400 V. Peak torque: 420 Nm. Max. Speed: 9000 rpm.
SRM	■ Cheap, simple, and rugged construction. ■ Rotor is composed of iron material. ■ Excellent torque–speed characteristics, which simplify control. ■ Fault-tolerant operation.	■ Increased weight compared with IMs and PMSMs. ■ High acoustic noise due to the high torque ripple. ■ High electro-magnetic interference (EMI). ■ Power is lower than PMSM and IM.	■ Model: 2013 Land Rover 110 Defender. Technology: SRM. Max. Power: 70 kW. Voltage: 300 V. Peak torque: 110 Nm. Max. Speed: 5400 rpm.

The power electronics topology of the EV traction inverter is determined by the selected electric motor technology. For EVs based on PMBDC motors, the speed of the vehicle is controlled by regulating the torque delivered to the wheels, which is directly proportional to the DC motor's armature current [18]. An example of this EV type is the small light-duty Kewet Buddy produced between 2007 and 2013 in Norway [19]. The Kewet Buddy EV is operated by a 72 V/13 kW separately excited DC motor, which is controlled by an H-bridge circuit that enables four-quadrant operation (forward/reverse and motor/generator). The Kewet Buddy H-bridge motor controller supports regenerative braking by reversing the armature current during operation to recover the braking energy back to the 10 kWh battery.

For IM-, PMSM-, and BLDC-based EVs, the three-phase VSI is the most commonly used topology, which can provide either sinusoidal or pulsating voltages and currents [20]. SRM-based EVs usually employ asymmetrical half-bridge (AHB) converters [21]. The OBC is another power electronic converter fitted within the EV to ease the battery charging process, which plays a crucial role in promoting EV sales by reducing the customer's

anxiety about the charging time. If the EV power electronic converter is designed to support bidirectional power flow, it can enable several desired functions such as vehicle-to-grid (V2G), vehicle-to-home (V2H), vehicle-to-load (V2L), or vehicle-to-vehicle (V2L), if a proper control system is deployed [6].

The aforementioned EV structures depend on a specific design for each EV, which is difficult to scale up or down. For example, increasing the power level of an EV model requires changing significant components in the mechanical and electrical systems to match the new power level, which increases the design effort. Several EV companies such as Kia, Hyundai, and Volkswagen, are working on modularising their future EVs by providing the so-called Global Modular Platform (GMP) for BEVs [22–24]. The GMP will enable EV companies to develop standard units that can be used to customise the EV design based on power level. This means that the units used for building small light-duty EVs can be used to build large electric buses, depending on the number and the connection of these units. This game-changer concept can reduce vehicle costs by sharing the same components among different models. Also, it can reduce the time required for designing and testing the new models and simplify production processes. Importantly, supply chain problems can be minimised and the time to release EVs to market can be reduced. On the downside, it is expected that the GMP will produce less optimised designs for specific applications and conventional non-standardised concepts will still be needed [22–24].

Despite the debate about aspects of the future of the GMP in the EV industry, modular power electronic converters and propulsion systems are required for future EVs replacing conventional VSI architectures. The modular systems employ several smaller electrical components connected and controlled together in a decentralised structure rather than depending on a centralised system [25]. An example is the modular multilevel converter (MMC), which replaced the VSI in several applications in either drive or renewable energy systems [26]. Modular systems provide advantages such as standard design, scalability, fault-ride-through capability, improved power quality, and better controllability. Adversely, modular structures increase the complexity of both hardware connection and software control systems [27].

To provide an insightful overview for researchers and engineers working on the GMP of EVs, this paper reviews the most important emerging modular topologies that can shape the future of the next EV generation. This paper reviews these modular topologies from the following four aspects: battery architectures, propulsion systems, charging infrastructure, and electric machines.

In the remainder of this paper, Section 2 the modular converter topologies used in battery systems will be discussed. In Section 3, the modular propulsion systems will be presented and discussed. The power converter architectures used in OBC, fast chargers, and V2G modes will be presented in Section 4. The promising topologies for modular cascaded machines applied within EVs will be discussed in Section 5. Some important points obtained from this review will be presented and discussed in Section 6, while the conclusions and findings drawn from the discussions will be presented in Section 7.

2. EV Modular Battery Systems

The first attempt to modularise the battery system of a hybrid EV (HEV) was published in [28], where the cascaded H-bridge (CHB) converter is employed to connect 48 V battery modules to the electric motor of the propulsion system, as shown in Figure 2. The CHB is operated as a multilevel converter to generate near-sinusoidal waveforms at relatively low switching frequencies. An advantage of this system is that the battery packs are clustered in relatively low voltage groups to provide safer operation and wiring. The main drawback of this configuration is that the half-bridge (HB) modules draw discontinuous currents from the source, which is battery packs. Discontinuous current can adversely affect battery cell performance and reduce their lifetime. To deal with this issue, large electrolytic capacitors are used to filter input currents, which increase the size and reduce the system's reliability, contradicting the intended goal.

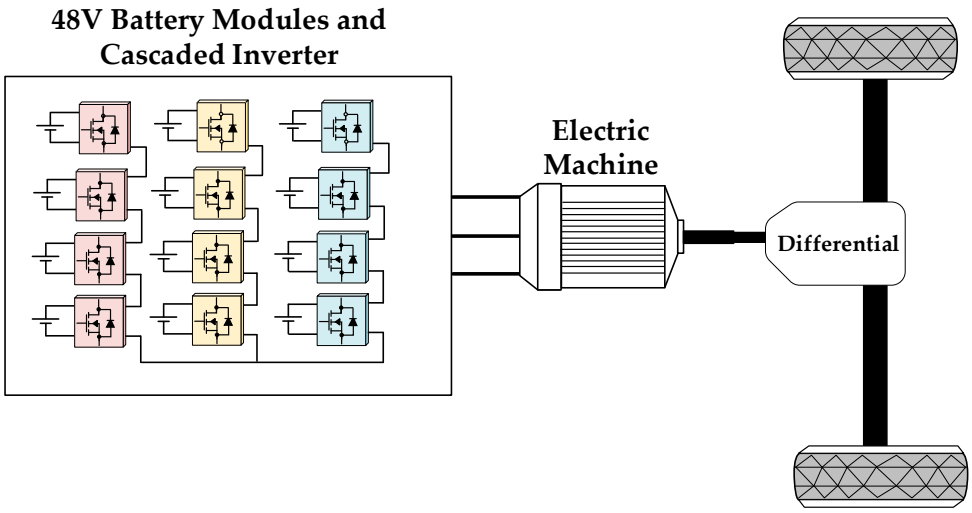

Figure 2. The EV cascaded multilevel converter in [28].

In [29], a modular architecture is proposed by connecting bypassing isolating DC/DC converters in parallel with battery strings. DC/DC converters are used to balance the battery strings together at the input sides and supply the LV auxiliary battery and loads at the output sides. Thus, the mismatch charge and energy between the battery strings is not wasted but instead is used to supply the auxiliary loads, as shown in Figure 3.

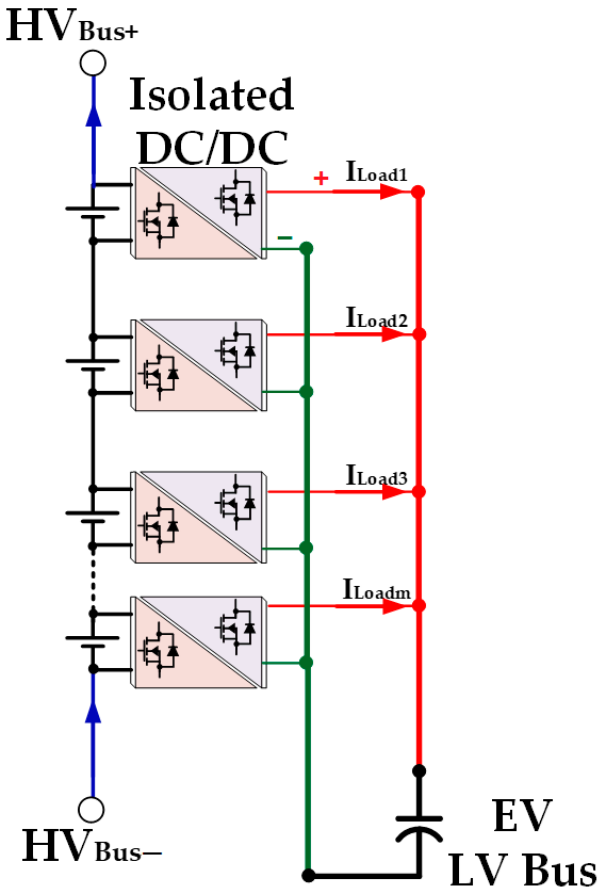

Figure 3. A modular architecture to balance HV battery cells using isolated bypass converters connected to an LV bus [29].

Dual active bridge converters are employed as an isolated DC/DC converter to support bidirectional power flow and also reduce the high-frequency isolating transformer size. Figure 4 shows the DAB structure with switch gate signals and main waveforms. As an advantage, DAB converters operate independently without the necessity for intercommunication. The research provided the control design for each isolated DC/DC converter but did not provide overall system control details needed to balance the battery strings' state of charge (SoC).

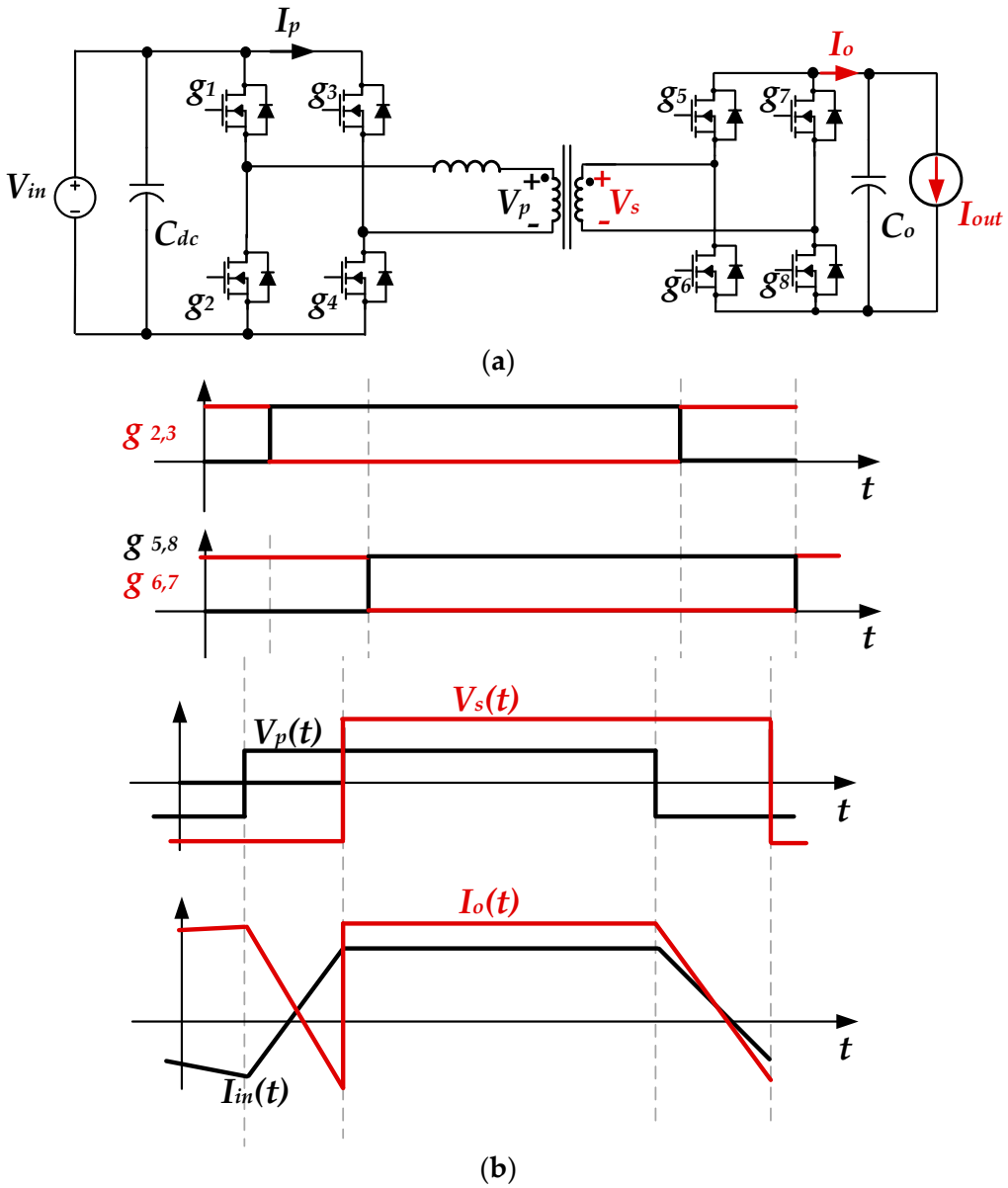

Figure 4. DAB unit in [29]: (**a**) circuit diagram and (**b**) gate signals, voltages, and currents.

The MMC in [30] is proposed to operate EVs with an SRM as the propulsion motor. The decentralised battery segments are connected to individual asymmetrical half-bridge converters, as shown in Figure 5. The first modular stage in Figure 5a is responsible for a series that adds the battery packs' voltages to form the dc-link voltage. The second stage in Figure 5b generates the required voltages and currents for the SRM. The two-stage configuration provides an additional system degree of freedom, controlling both the battery's as well as the machine's sides. The proposed asymmetrical MMC improves EV fault-ride-through capability, provides flexible DC bus voltages, and improves the THD of

the motor's voltages and currents. On the downside, the research did not provide details regarding the battery SoC balance. Also, the machine side stage in Figure 4b is not modular, which reduces the intended degree of scalability.

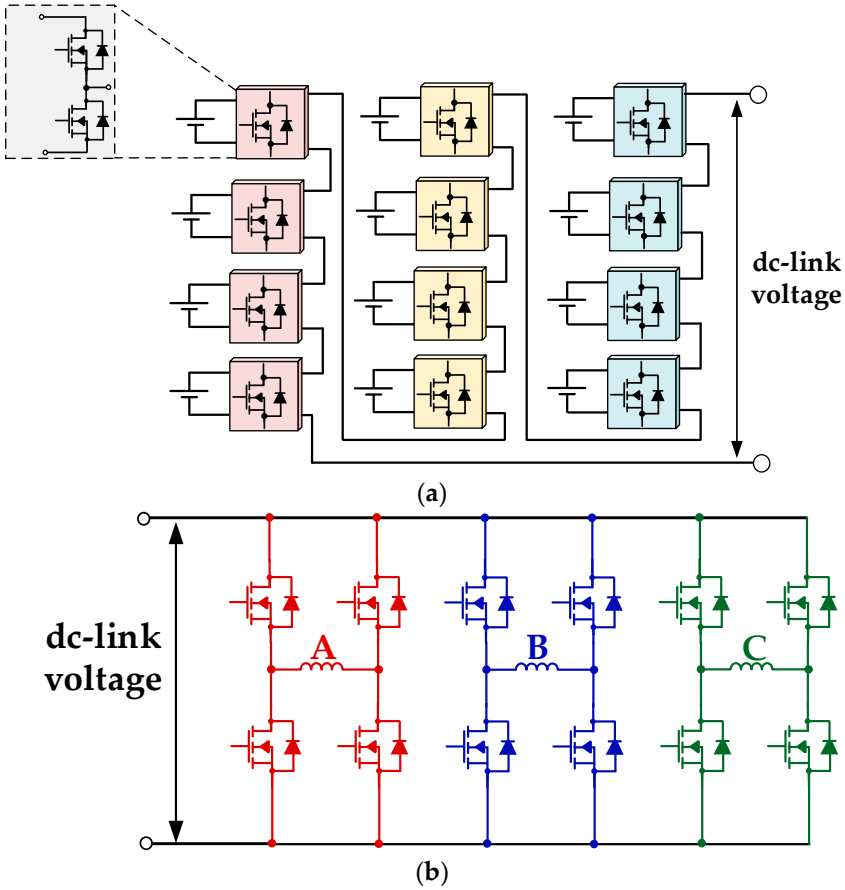

Figure 5. MMC with a decentralised battery storage system: (**a**) overall structure and (**b**) SRM drive in [30].

Reference [31] attempts to present an accurate model of the CHB modular architecture presented in [28] with a focus on the low-order current harmonics drawn by the battery segments. The paper applied the model to a seven-level CHB modular converter and compared the results during different driving cycles. The research concluded that the conventional pure resistive model overestimates the power losses by around 20%. So, the paper presented a dynamic three-time constant model using several RC-links, which were implemented and applied online to provide an accurate measure of battery power losses. The simulation model is based on numerical computer tools including the MATLAB/SIMULINK and MATLAB curve-fitting toolbox.

The modular converter in [32] employs two-stage submodules (SMs) with each battery segment as shown in Figure 6. The first stage is based on an isolated Sepic converter, which can draw a continuous current from the battery packs and provide galvanic isolation between the battery and the dc-link. The second stage is based on a full-bridge two-level converter to shape the output voltage and current based on the mode of operation. The modular architecture can provide decentralised control of the battery segments according to SoC and temperature. The proposed MLI is designed to operate in normal driving, regenerative braking, and charging modes. The good controllability of the proposed system comes at the expense of a complicated control scheme.

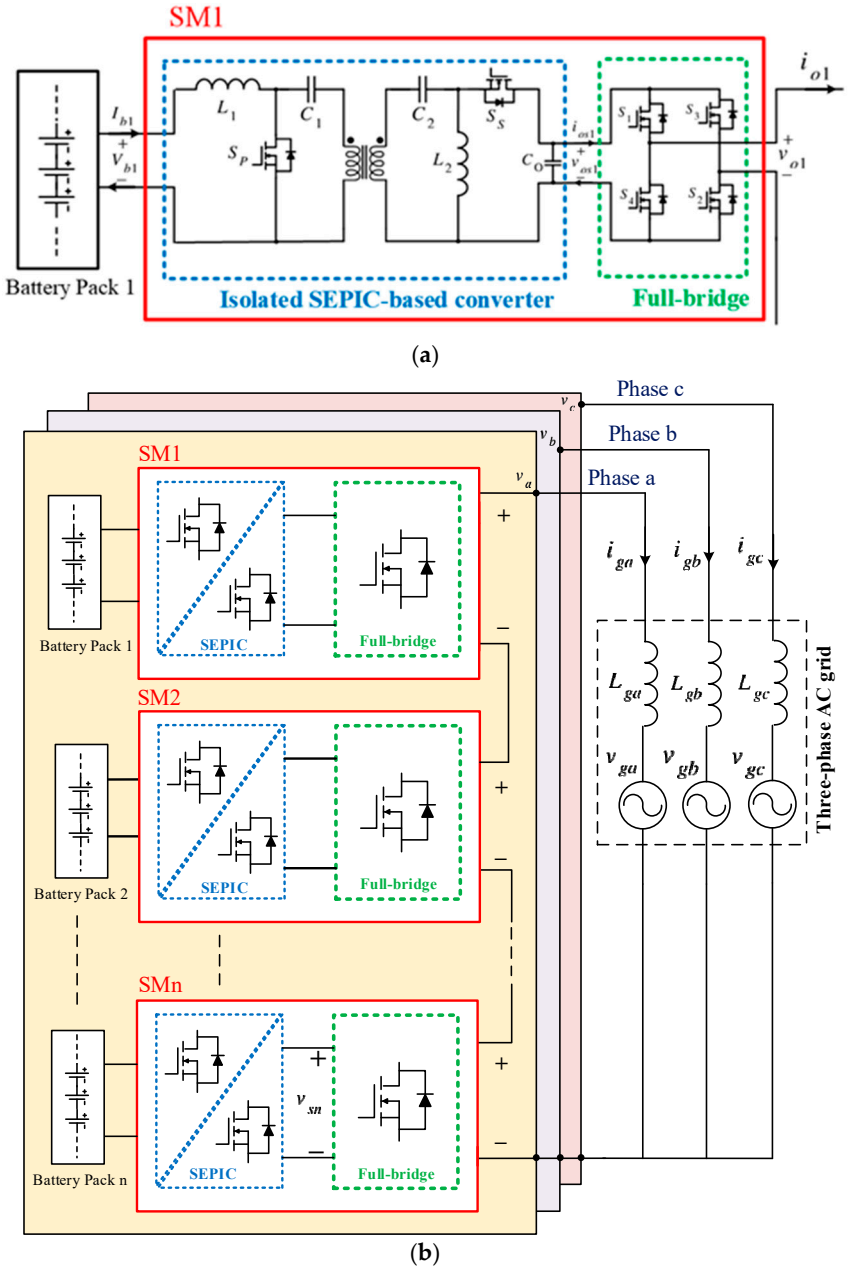

Figure 6. Modular FB/Sepic converter [32]. (**a**) single SM; (**b**) full system.

Table 2 summarises the reviewed EV modular battery systems.

Table 2. Summary of the reviewed EV modular battery systems.

Refs.	Topology	Machine	Power	Switching Freq.	Year	Remarks
[28]	CHB	—	1.5 kW	300 Hz	2002	Needs large capacitors
[29]	DAB	—	2 kW	200 kHz	2016	HV battery balancing Complicated control design
[30]	MMC/AHB	SRM	0.75 kW	—	2019	Online balancing of battery packs
[31]	CHB	—	—	—	2020	Accurate model for low-order harmonics in battery currents
[32]	Sepic/FB	PMSM	3 kW	20 kHz	2024	Driving modes are studied with respect to battery temperature

SIMULINK/MATLAB 2024a models are used to show the key CHB system waveforms in [28], the decentralised EV battery system for SRMs in [30], and the SEPIC-based integrated OBC system in [32]. The three models employ the same MOSFET and diode devices, while the passive inductors are selected so the current ripple gives an output THD below 5%. Figure 7 shows the total output voltage, total output current, and one battery current in the first SM of each system. These sample waveforms are taken at an SM battery voltage of 50 V and a switching frequency of 5 kHz. Figure 8 shows the efficiency plots of each modular battery system where the single-stage CHB has the highest, followed by the SEPIC-based system in [32] with the lowest efficiency for the SRM-based system in [30].

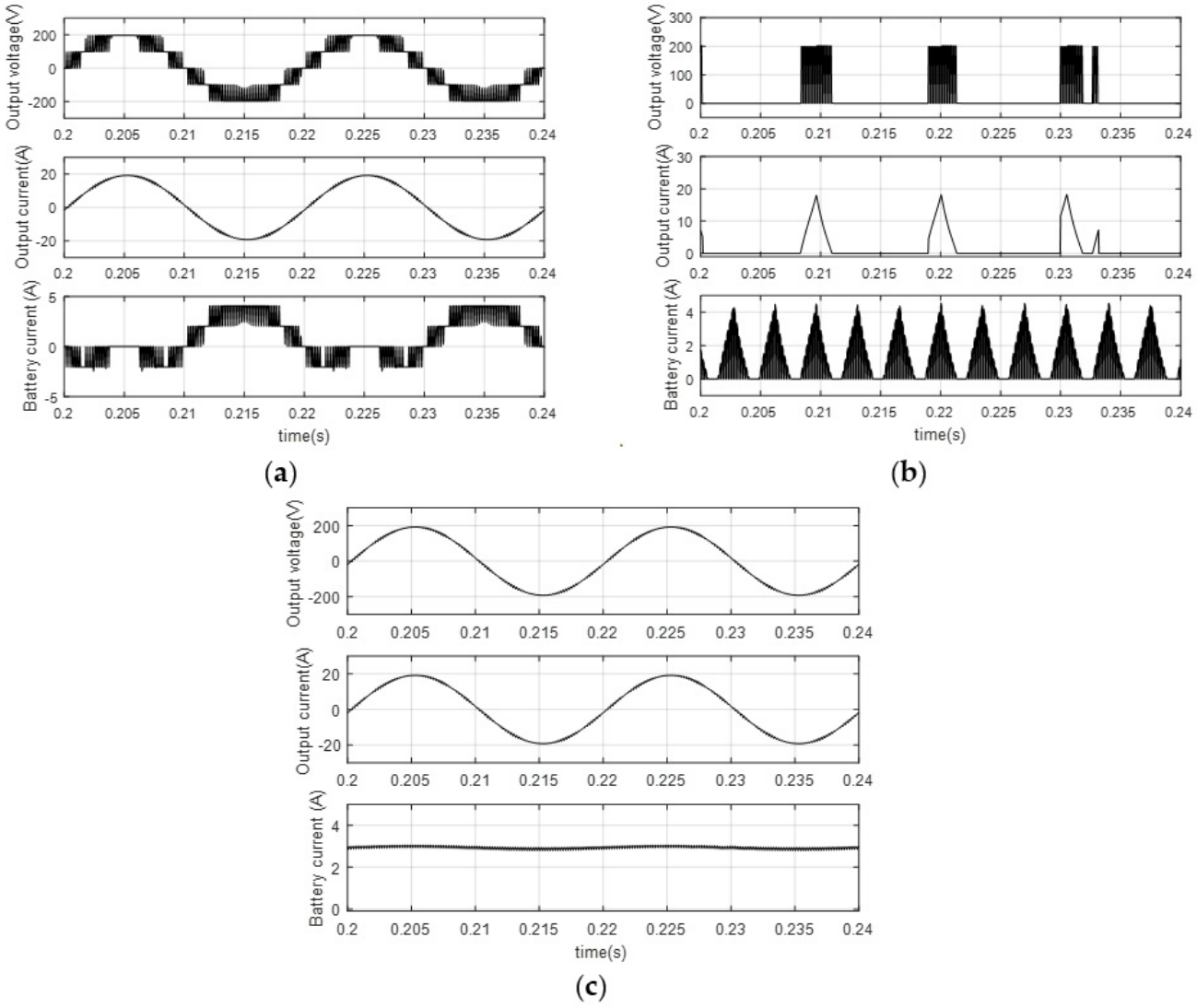

Figure 7. Modular battery system waveforms: (**a**) the modular CHB system in [29], (**b**) the modular SRM-based system in [30], and (**c**) the SEPIC-based integrated charger in [32]. (Top: output voltage, middle: output current, and bottom: battery current in a single SM).

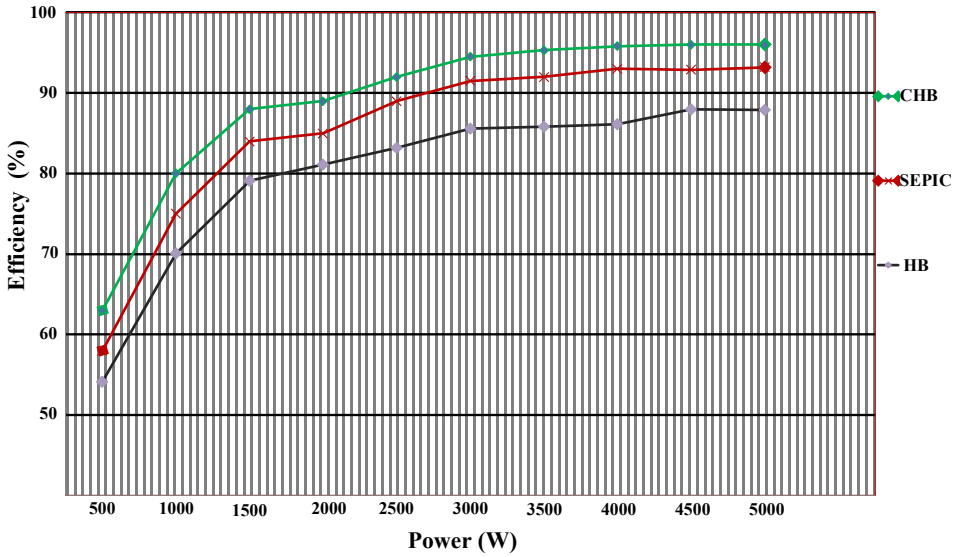

Figure 8. Efficiency comparison for modular battery systems (green: [29], red: [30], and black: [32]).

3. Modular Propulsion Systems

Modularising the power electronic converter in the EV propulsion system was proposed first in [33] with a cascaded DC/AC H-bridge MMC. As shown in Figure 9, the DC source is connected to the H-bridge cells through a VSI. This boosts the DC voltage, which provides better control without the need for bulky inductors. However, the operation and dynamic response of the proposed MMC with the machine were not presented.

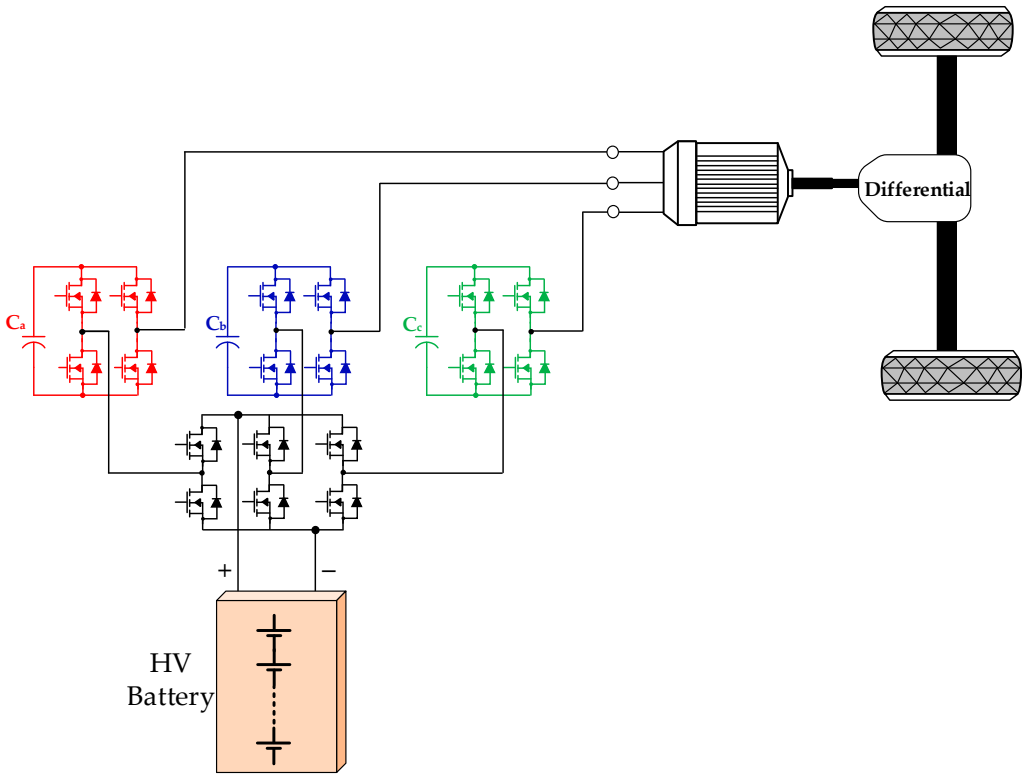

Figure 9. The DC–AC cascaded H-bridge multilevel boost inverter in [33].

In [33], traction inverter operation was examined using SIMULINK/MATLAB computer simulation during acceleration, constant-speed operation, and deceleration. Figure 10a shows the velocity profile tracked over a duration of 20 s, while Figure 10b shows the actual speed

and motor torque. Figure 10c shows the motor phase voltage with the input current from the battery during the acceleration period. The simulation component parameters are listed in Table 3.

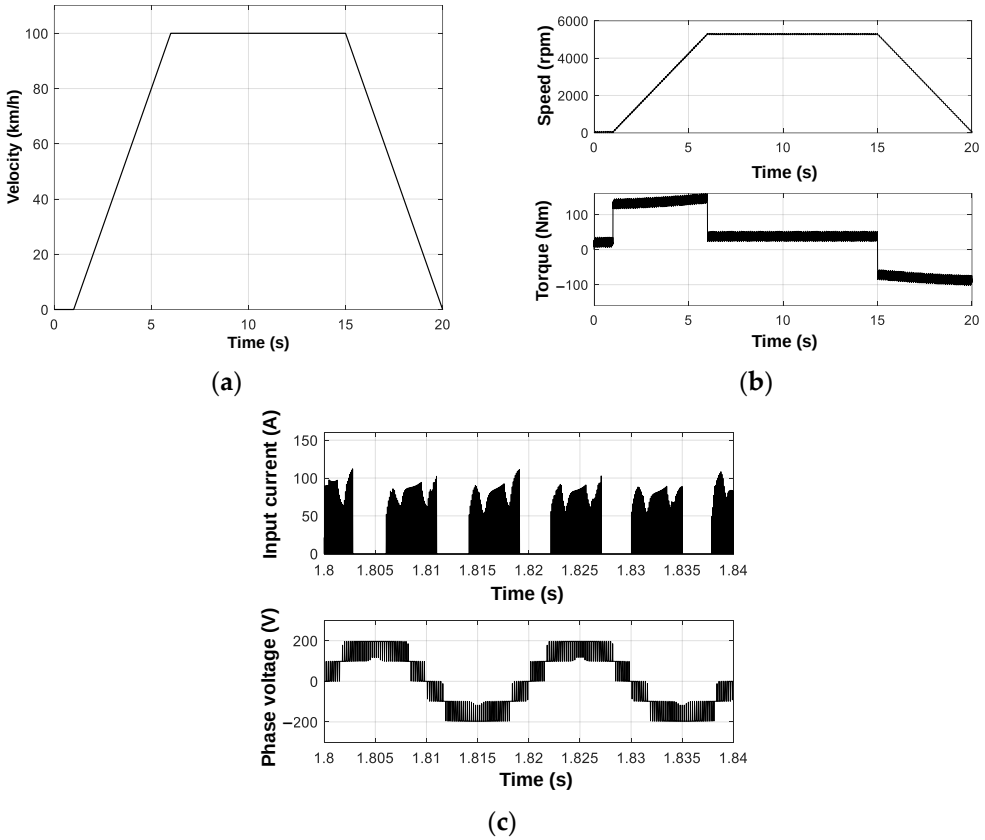

Figure 10. MATLAB simulation waveforms of the modular traction inverter in [33]: (**a**) reference velocity profile, (**b**) motor speed and torque, and (**c**) acceleration phase voltage and battery current.

Table 3. System parameter values in the MATLAB simulations.

Parameter	Value
Switching frequency	5 kHz
Battery voltage	400 V
Motor	PMSM
No. of poles	10
No. of levels	4
Motor inductance	$L_d = L_q = 0.28$ mH
Phase resistance	$R_s = 0.2\ \Omega$
EV mass	300 kg
Differential ratio	1:4
Wheel radius	30 cm

The research in [34] studied the feasibility of using an asymmetrical CHB inverter when SMs do not necessarily have the same size and volume. The isolated converter shown in Figure 11 can minimise the size of the isolating high-frequency transformers (HFTs) and operate some of the SMs as active filters with small cores. In this way, the number of DC supplies needed to operate the system is reduced and the greatest portion of power is transferred through the larger H-bridge SMs. The operation of the 27-level converter was tested using an 18 kW EV prototype.

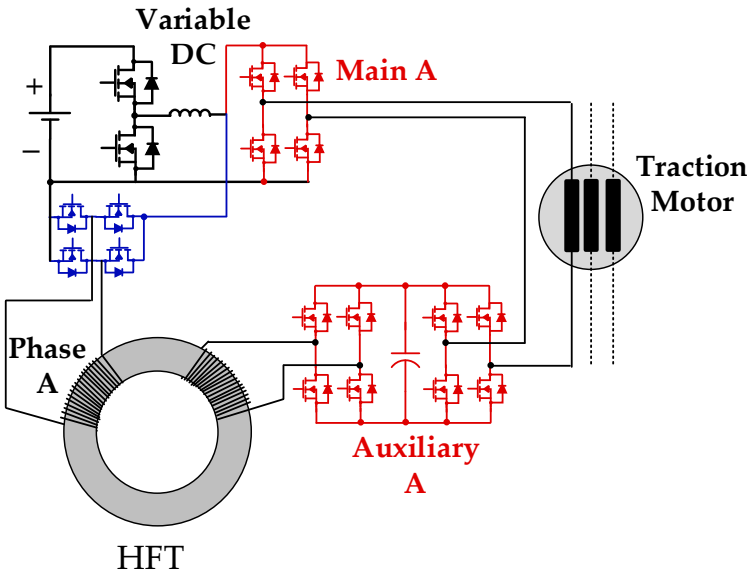

Figure 11. Topology for one phase of the asymmetrical CHB with HFT in [34].

Figure 12a shows the actual speed and motor torque when simulated using MATLAB at the same conditions listed in Table 3 and the velocity profile in Figure 10a. Figure 12b shows the motor phase voltage with the auxiliary stage current.

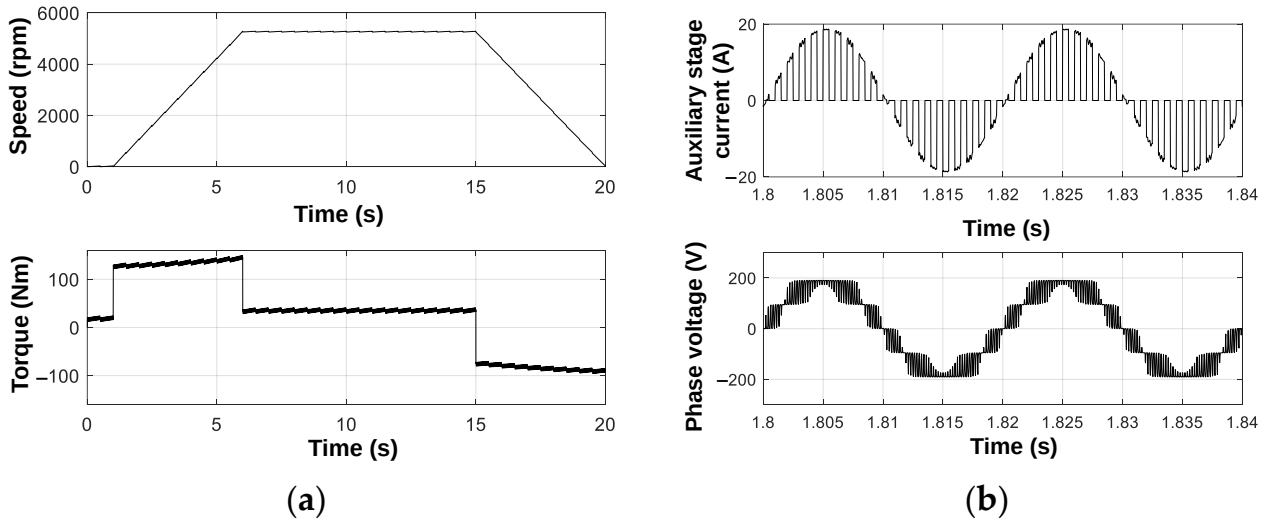

Figure 12. MATLAB simulation waveforms of the modular traction inverter in [34]: (**a**) motor speed and torque, and (**b**) acceleration phase voltage, auxiliary current, and battery current.

The proposed converter in [35] is an extension to the MMC-based drive for SRMs by modifying the front-end circuit to provide flexible energy conversion and BMS. As shown in Figure 13, the cascaded multiport converter integrates the battery packs into the asymmetric half-bridge converter. The battery packs are split into three phases to provide fault-tolerance and regenerative braking capabilities. The current regulator is based on hysteresis control, which can increase the noise in the system especially when the SRM has low inductance and inertia.

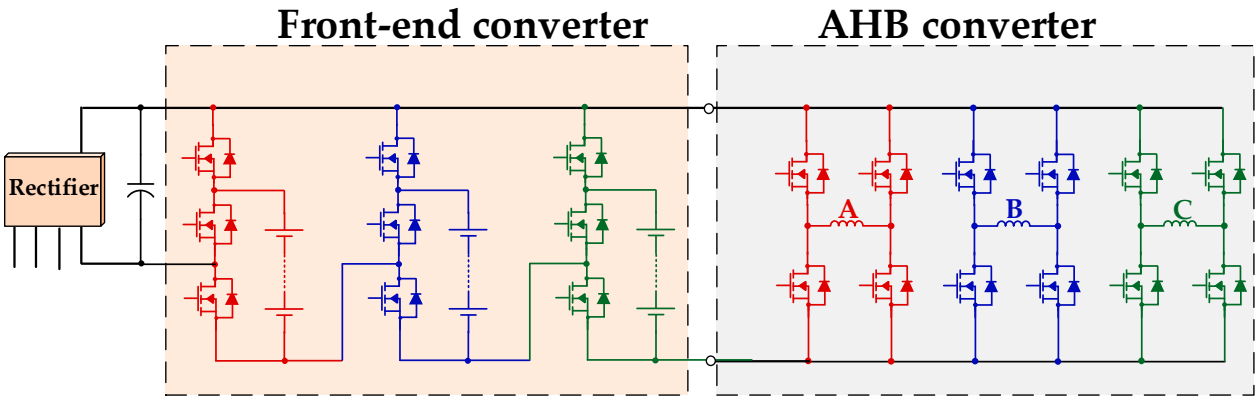

Figure 13. Cascaded multiport converter for a three-phase SRM [35].

Power and signal multiplex transmission (P&SMT) is proposed in [36] to provide both power transfer and communication signal transmission in the same converter. As shown in Figure 14, the converter can transmit the measurements and control signals without the need for a controller area network (CAN), aiming to reduce the wiring in the EV. Also, the converter aims to adjust the motor speed and battery balance during the EV's normal operation.

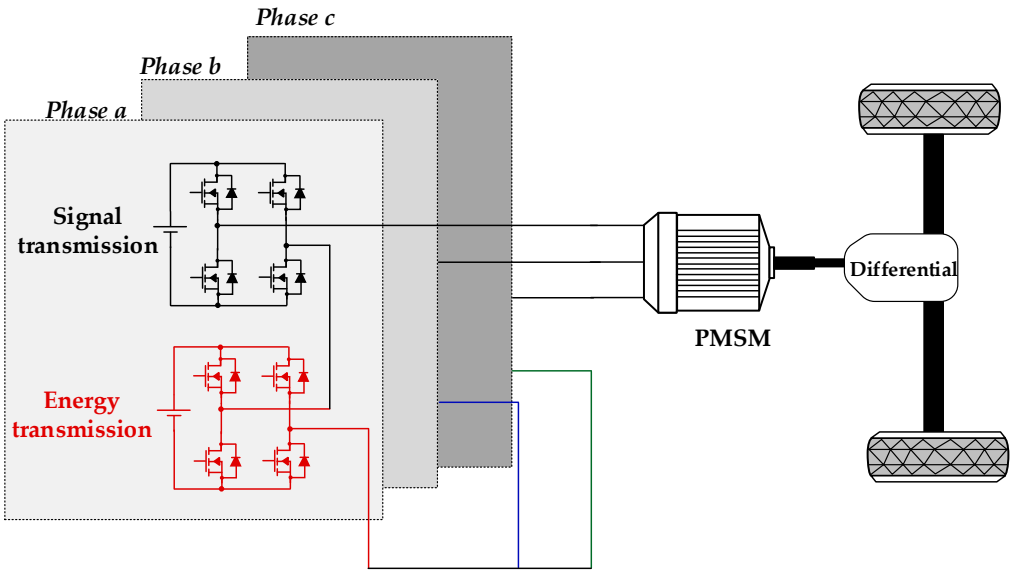

Figure 14. The power and signal multiplex transmission for EVs in [36].

A model predictive control (MPC) system for the MMC in the context of EV is proposed in [37] with different SM cells to track the current motor error while reducing the switching frequency of the devices. The proposed controller aims to provide a better integration of the decentralised cells into the EV drivetrain. The speed controller in Figure 15 still uses a conventional proportional-integral-derivative (PID) controller, which generates the reference torque to the maximum torque per ampere (MTPA) block, which in turn generates the reference three-phase current. The MPC algorithm then uses the information about the current, voltage, and battery SoC to generate the gate signals required to operate the MMC.

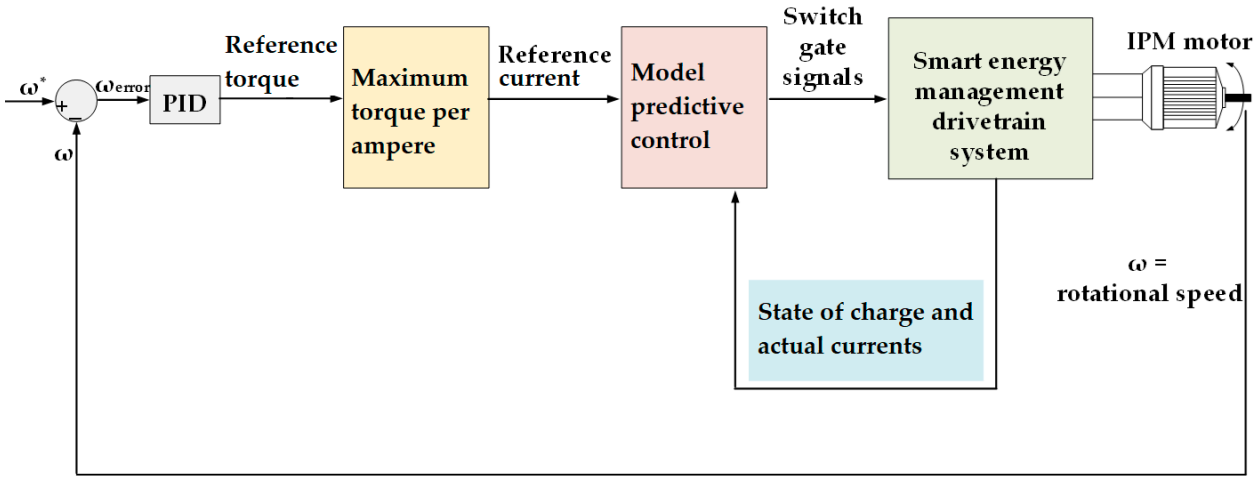

Figure 15. Model predictive control-based controller for EV drivetrains in [37].

In [38], a five-level modular boost inverter based on a T-type converter is presented and tested experimentally to reduce the imbalance across T-type converters. Accordingly, small capacitors can be employed rather than large electrolytics to reduce the size and weight of the total system. The proposed system in Figure 16 is a DC/DC boost stage to boost the battery's voltage, followed by a modular DC/AC stage to shape the motor's voltage and current. During boosting, the voltage stresses across the devices in the first stage might be high, thus needing a special design.

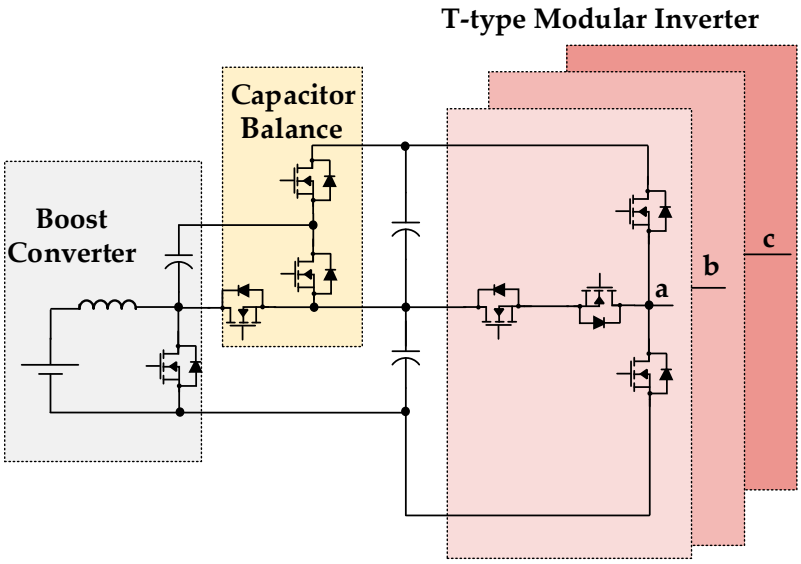

Figure 16. Modular bidirectional boost DC-DC converter with a T-type inverter [38].

Figure 17a shows the simulation results for the T-type inverter when used as a traction inverter to a PMSM with parameters listed in Table 3 and the velocity profile in Figure 10a. The actual speed and motor torque are shown in Figure 17a, while the input current of the boost stage, the middle stage voltages, and the output phase voltage are shown in Figure 17b.

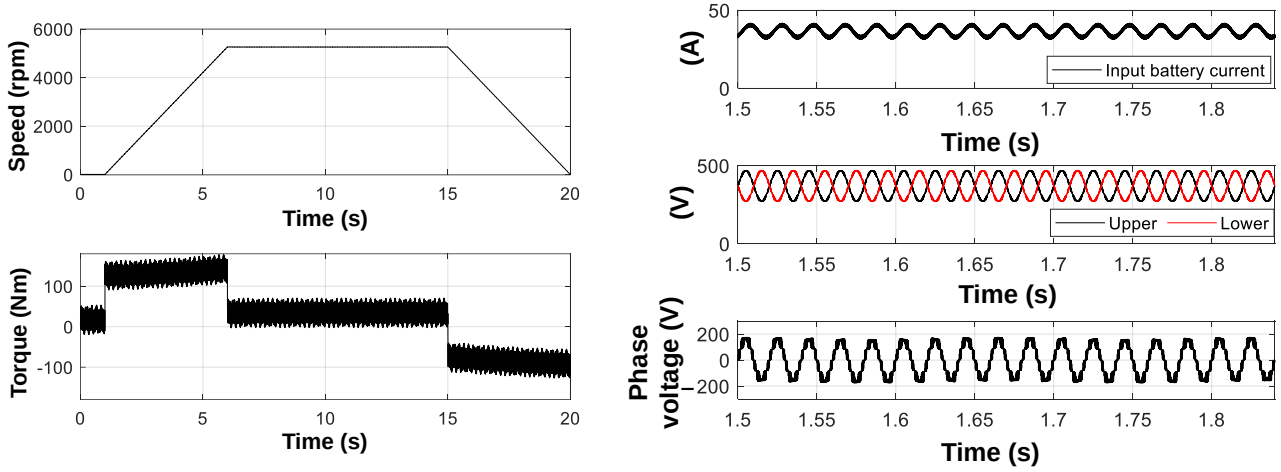

(**a**) (**b**)

Figure 17. MATLAB simulation waveforms of the T-type traction inverter in [38]: (**a**) motor speed and torque, and (**b**) acceleration input current, middle capacitor voltages, and battery input current.

The efficiency of the propulsion inverters with PMSMs in [33,34,38] are simulated using the same method and conditions as in Section 2. The efficiency plots in Figure 18 show that the CHB-based modular inverter in [33] has the best efficiency at the same conditions regardless of the power range. Second, the efficiency of the T-type modular inverter in [38] is better than that of the isolated asymmetrical CHB modular traction inverter in [34].

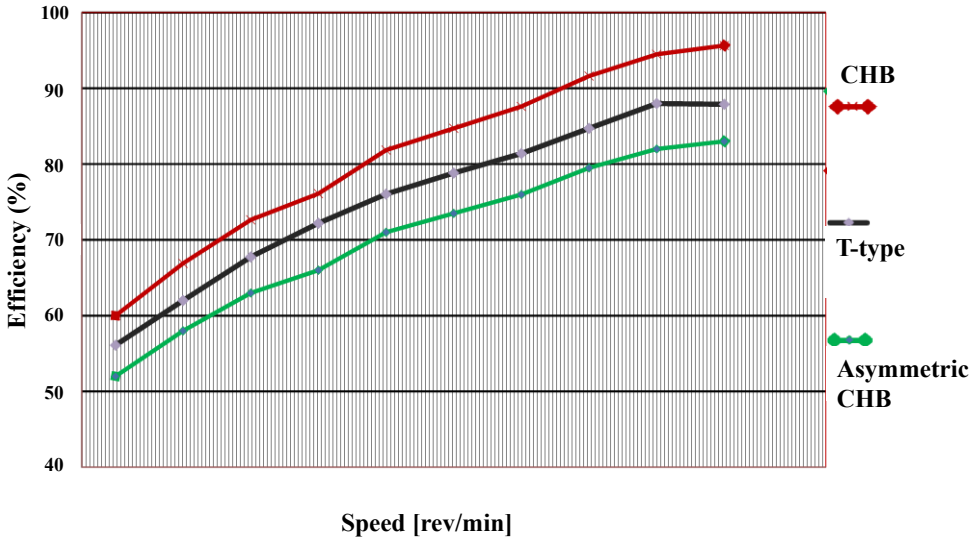

Figure 18. Efficiency comparison of modular traction inverters (red: [33], black: [34], and green: [38]).

An isolated modular multilevel bidirectional DC/DC converter is presented in [39] to boost a battery's LV to match the level of the HV propulsion inverter. As shown in Figure 19, the modified two-split capacitor half-bridge (HB) circuits are connected in a series/parallel configuration to increase the voltage at the DC side of the inverter. As the proposed converter is bidirectional, it can reverse the power flow during regenerative braking to charge the batteries using the full-bridge (FB) converter. The system benefits from the zero voltage switching (ZVS) capability to reduce the semiconductor power losses and improve the total efficiency to above 95%. The operation of the proposed high-gain converter is tested in the DC/DC mode at 1.5 kW but not with a specific inverter or motor during driving and braking modes.

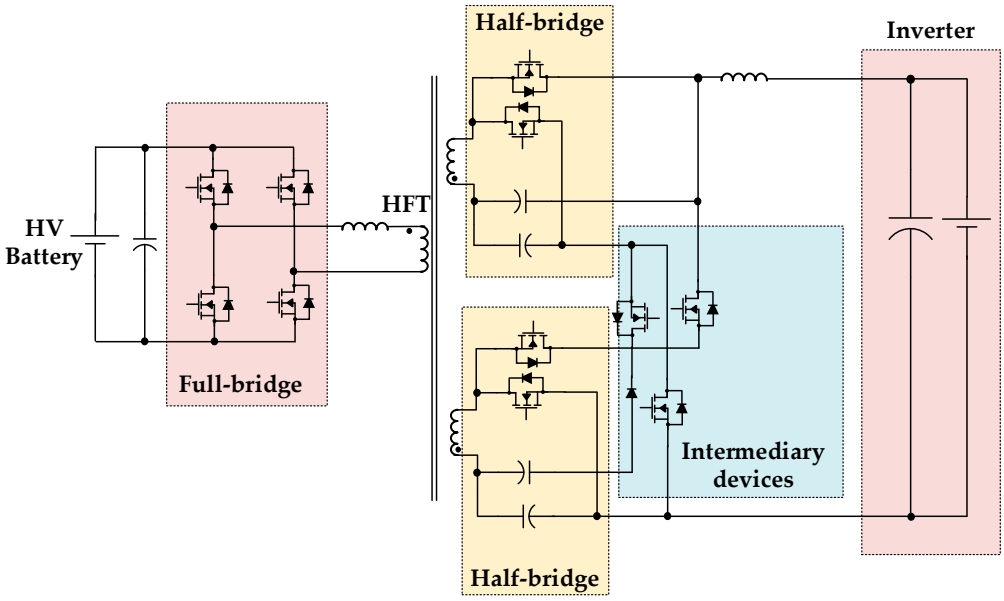

Figure 19. Bidirectional modular DC-DC converter in [39].

A summary of the reviewed traction inverters is shown in Table 4.

Table 4. Summary of the reviewed EV modular propulsion systems.

Refs.	Topology	Machine	Power	Switching Freq.	Year	Remarks
[33]	CHB	—	5 kW	—	2009	Needs a central VSI at the DC source
[34]	ACHB	BLDC	18 kW	5–20 kHz	2012	Complicated HFT design
[35]	AHB	SRM	1 kW	5 kHz	2019	Driving/braking modes are presented
[36]	P&SMT	PMSM	—	2 kHz	2020	Simulation-based
[37]	MMC	IPM	3.5 kW	—	2022	MPC control
[38]	T-type	—	1 kW	5 kHz	2019	Challenging design of the input boost converter at high power
[39]	FB/isolated	—	1.5 kW	50 Hz	2022	Provides a high DC/DC voltage boosting ratio

4. Modular Charging Systems

Figure 20 shows the main EV charging systems including OBCs, wireless charging, and off-board charging. OBCs are classified into Level 1 and Level 2 chargers. Level 1 provides slow charging at 3.7 kW with a single-phase 120–230 VAC input voltage. Level 2 usually operates with three phases, where the power level can reach 22 kW. Level 3 fast chargers usually operate at a three-phase AC input voltage where the charging power can exceed 50 kW and reach 300 kW.

The two-stage converter is a common OBC topology in modern EVs, where the first stage rectifies the input AC voltage using an AC/DC rectifier and the second stage regulates and controls the HV battery current using a DC/DC converter [32].

The same types of topologies at different power and voltage levels are designed for DC fast chargers, wireless charging, and V2G converters. To increase the power level and improve charging system reliability, modular and multiport topologies have been proposed in the literature for medium-voltage AC (MVAC) and medium-voltage direct current (MVDC) charging stations and off-board fast DC chargers.

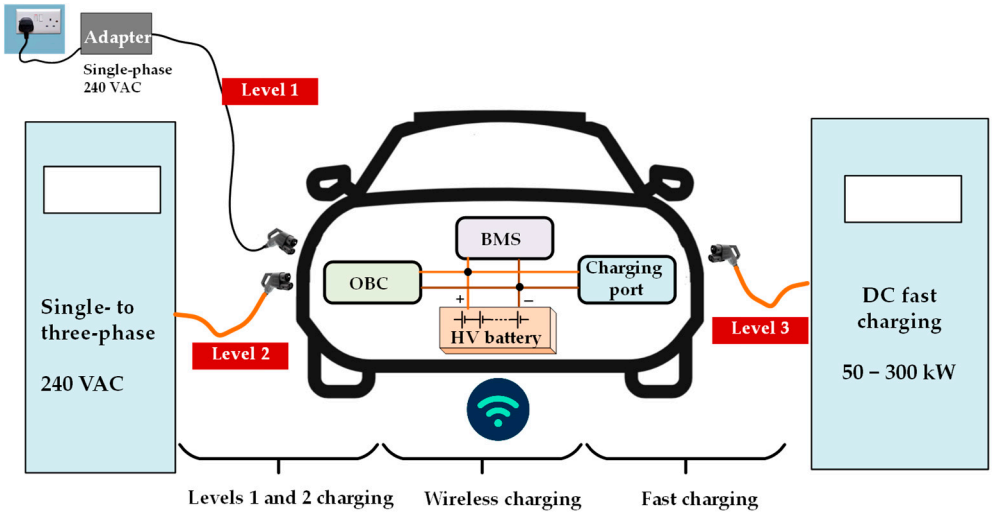

Figure 20. Main charging levels of EVs.

4.1. MV Charging Stations

The conventional power distribution system for a large-scale charging infrastructure is shown in Figure 21, where MV/LV transformers are used to integrate the charging units into the MV AC grid. In such systems, the internal LVAC buses with transformers are used to supply groups of chargers. These LVAC buses usually carry high currents and hence, the cables have a large cross-section area resulting in increased weight and size.

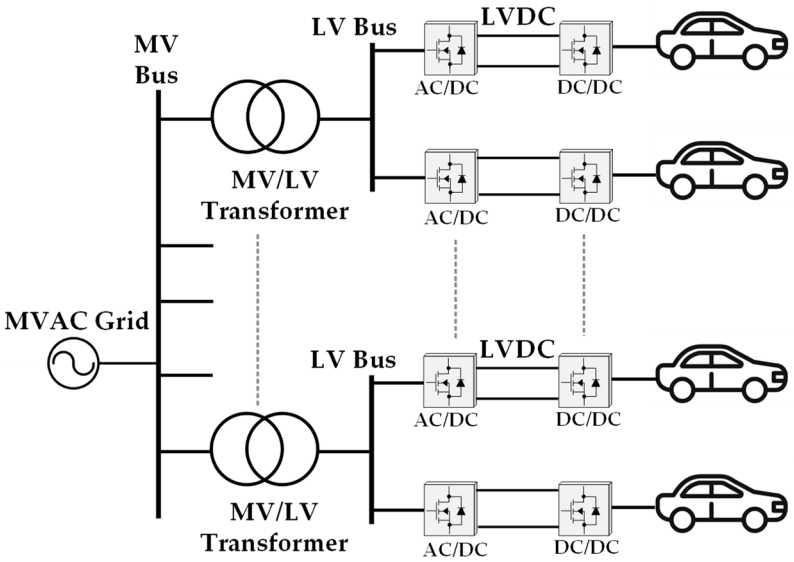

Figure 21. Conventional power distribution system for large-scale charging infrastructure.

MMC structures in the literature aim to reduce the footprint of MVAC charging stations [40–42]. As shown in Figure 22, the MMC-based topologies in [40,41] allow for charging station connection to the MVAC without the necessity for a large MV transformer, benefiting from internal high-frequency transformers (HFTs) in the SMs. Also, the system provides a high degree of freedom during charging as the SMs can be controlled individually. The main challenge in this configuration is to control the circulating currents in the three phases, especially with heavy unbalanced charging and unequal loading.

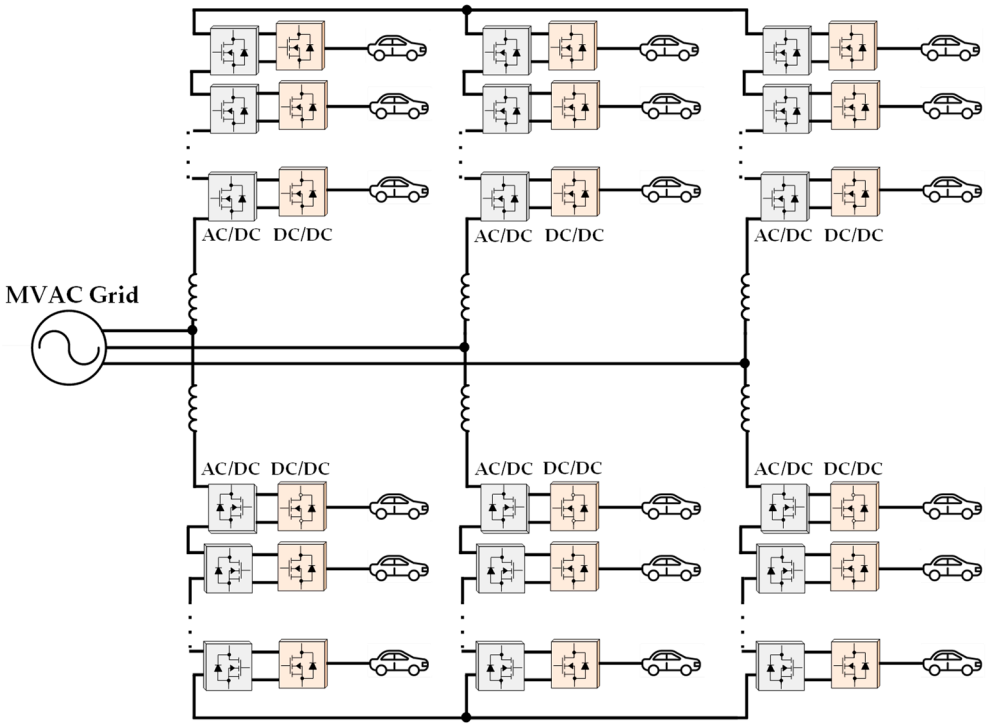

Figure 22. EV charging MMC-based grid interface connected to an MVAC grid [40,41].

The concept of a multiple active bridge (MAB) converter is studied in [42], where the DC/DC conversion part is modularised using dual active bridge (DAB) ports, as shown in Figure 23. The MAB system can deliver high charging power to EV batteries by providing a sort of galvanic isolation to comply with grid standards.

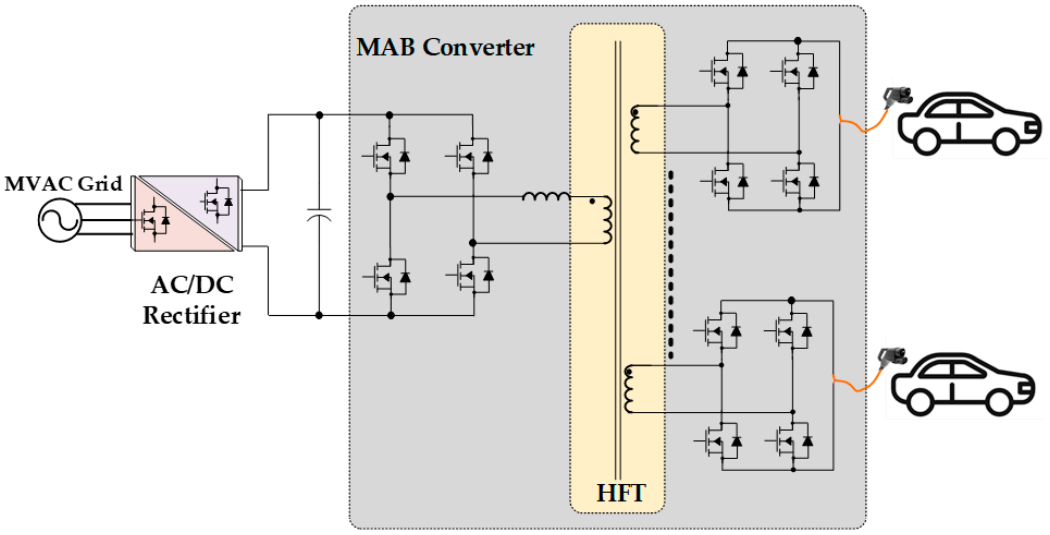

Figure 23. The MAB converter for EV charging with an MVAC grid interface in [42].

Note that although the MAB converter can share the charging power among the DAB SMs, the total input power delivered by the grid flows through the AC/DC rectifier and, therefore, it should be designed for a high power level.

With increased MVDC-based grid penetration, direct DC/DC charging stations have gained attention, especially with the availability of distributed energy sources and storage systems [43]. A multiple-output DC/DC MMC for EV fast chargers is proposed in [44]. As shown in Figure 24, the input terminals of the proposed converters are connected to the MVDC grid where the voltage is shared by HB cells. The modular output sides are

connected to the EV batteries through FB converters, with a voltage range of 400 V to 800 V. The medium-frequency modular transformer (MFMT) isolates the input and output and provides additional voltage ratio control when required. Because of the FB cells at the output sides, the modular converter has inherent DC fault-blocking capability, which is necessary for this application. The design and manufacturing of the MFMT is simple because of the HV level of the DC grid.

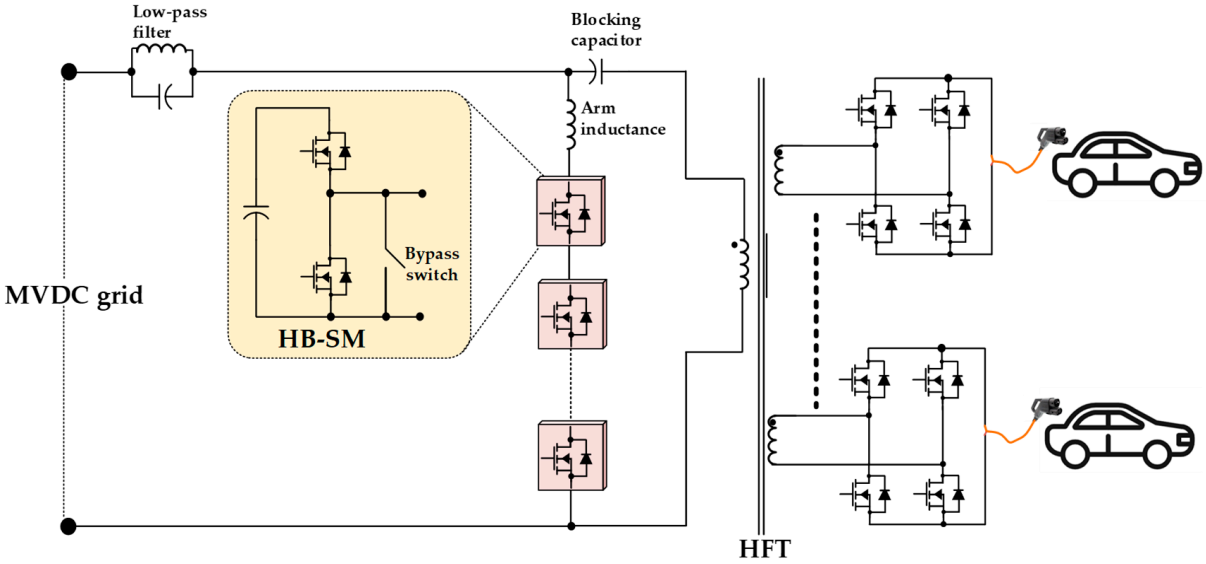

Figure 24. The MVDC MMC-based charger in [44].

4.2. Fast Interleaved Chargers

The term 'fast charging' is usually defined as chargers that can charge the EV battery from 20% to 80% in around 10 min, which can be achieved when the charger has a power rating of at least 50 kW [45]. Power converters can be connected in parallel, series, or parallel–series combinations to increase the EV charger power level. Interleaved configurations for DC/DC boost converters are employed to reduce the current and voltage ripple, especially when non-linear quasi-saturated inductors are used [46,47]. An example is the interleaved fast charger based on modular converters shown in Figure 25 [48]. In this system, several active interleaved rectifiers are connected to the three-phase AC mains, where their output terminals are connected in parallel to the dc-link capacitor. Then, parallel-connected DC/DC converters are used to regulate the battery charging process at high power. In this way, the converter output power can reach 150 kW with a possible increase to 300 kW if SiC MOSFETs are used. The interleaved connection enables reduced current ripple at the input and output sides, which can reduce the filtering inductor size and, therefore, the total weight of the charger. The converters can be controlled to allow for bidirectional power flow when the EV battery is required to support AC loads in V2G operation [49]. It is necessary to design a fast control system for the interleaved charger to avoid circulating currents among the parallel connected converters when the output voltages are not equal. The modular structure of interleaved fast chargers provides a beneficial redundancy during partial failure in any of the converters, as the charger can continue operating at lower power using suitable detection and control systems.

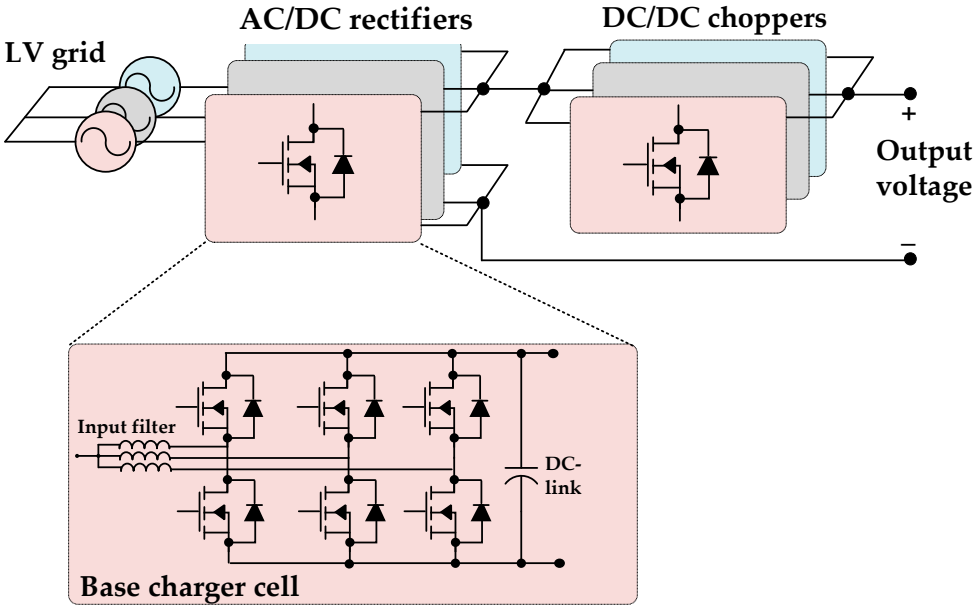

Figure 25. The EV fast charger based on three-phase interleaved converters in [48].

4.3. OBCs

The published modular OBC systems centre on the DAB converter as a building block. One reason is the galvanic isolation capability provided by the HFT between the input and output, which enables the OBC to comply with regulating standards such as IEC61851 and SAEJ1772. A benefit of galvanic isolation is that failures during charging can be detected by the isolation monitoring system (IMS); hence, the controller can use this information to initiate safe action [50]. Also, the DAB converter is capable of providing voltage buck–boost operation, which gives the system additional control if increasing the battery voltage is required.

A 22 kW modular OBC based on the DAB converter is presented in [51], as shown in Figure 26. The input of the DAB units (switches 1 to 4) converts the 50/60 Hz AC mains voltage to a high/medium frequency square wave voltage at tens of kHz. The output side (diodes 5 to 8) rectifies the square wave HF voltage into DC voltage to charge the HV battery. The efficiency of the DAB units is around 94.5% and does not fall significantly with increasing system voltage. The research recommends operation when the number of DAB units is increased to extend the power from 3.6 kW to 22 kW, but the effect on the grid current waveforms was not considered.

The OBC in [52] extends the previous converter to a three-phase operation where the output side of the DAB units incorporates anti-parallel switches with the diodes to enable bidirectional power flow. Reversing the power flow is needed when the OBC operates in V2G mode where the EVs can support the grid off-peak [53]. As shown in Figure 27, the large input electrolytic capacitors are eliminated by the introduction of input inductors. The three-phase operation and connection remove the second-order harmonics from the battery currents. Adversely, the OBC is not suitable for single-phase applications, which is not favoured by EV owners [53]. The zero voltage switching (ZVS) technique implemented for the OBC increases the efficiency to above 95%, which is crucial for the application.

The modular OBC shown in Figure 28 is suitable for single-phase operation where the input side incorporates an additional bridge [54]. The converter is modified to this configuration to decouple the second-order component from the battery current and hence avoids the generation of third-order harmonics in the grid current, which can negatively affect operation. An efficiency of 91.4% during normal charging and 90.1% during the V2G mode was reported. Table 5 summarises the reviewed modular charging systems.

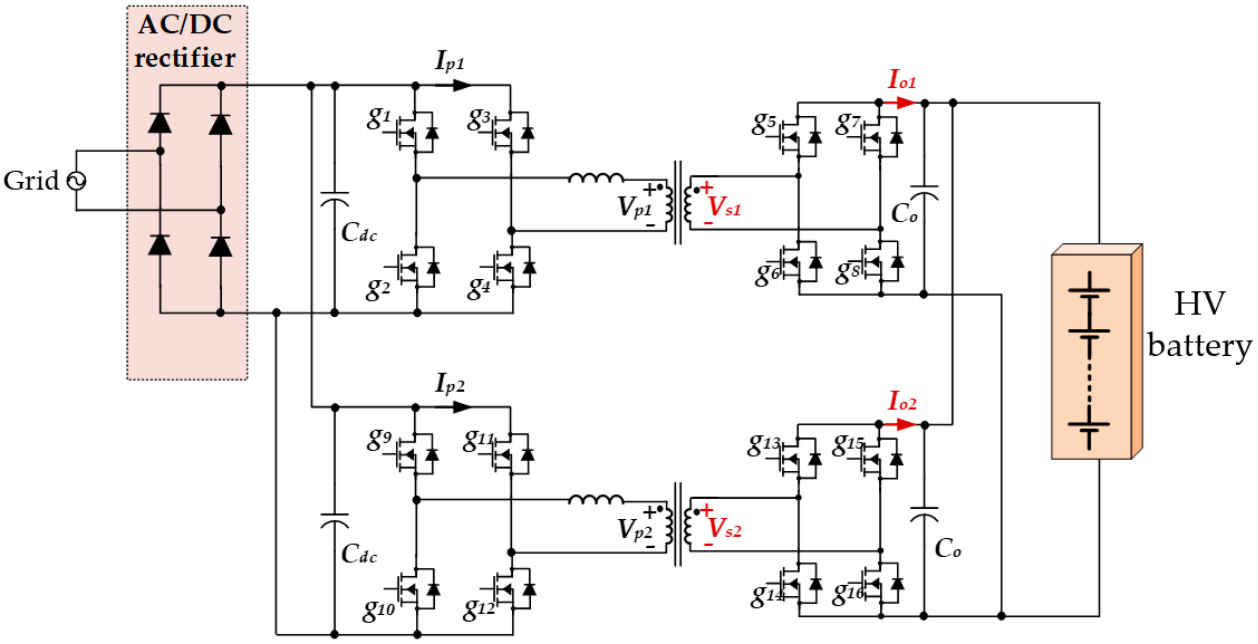

Figure 26. A 22 kW OBC based on DAB in [51].

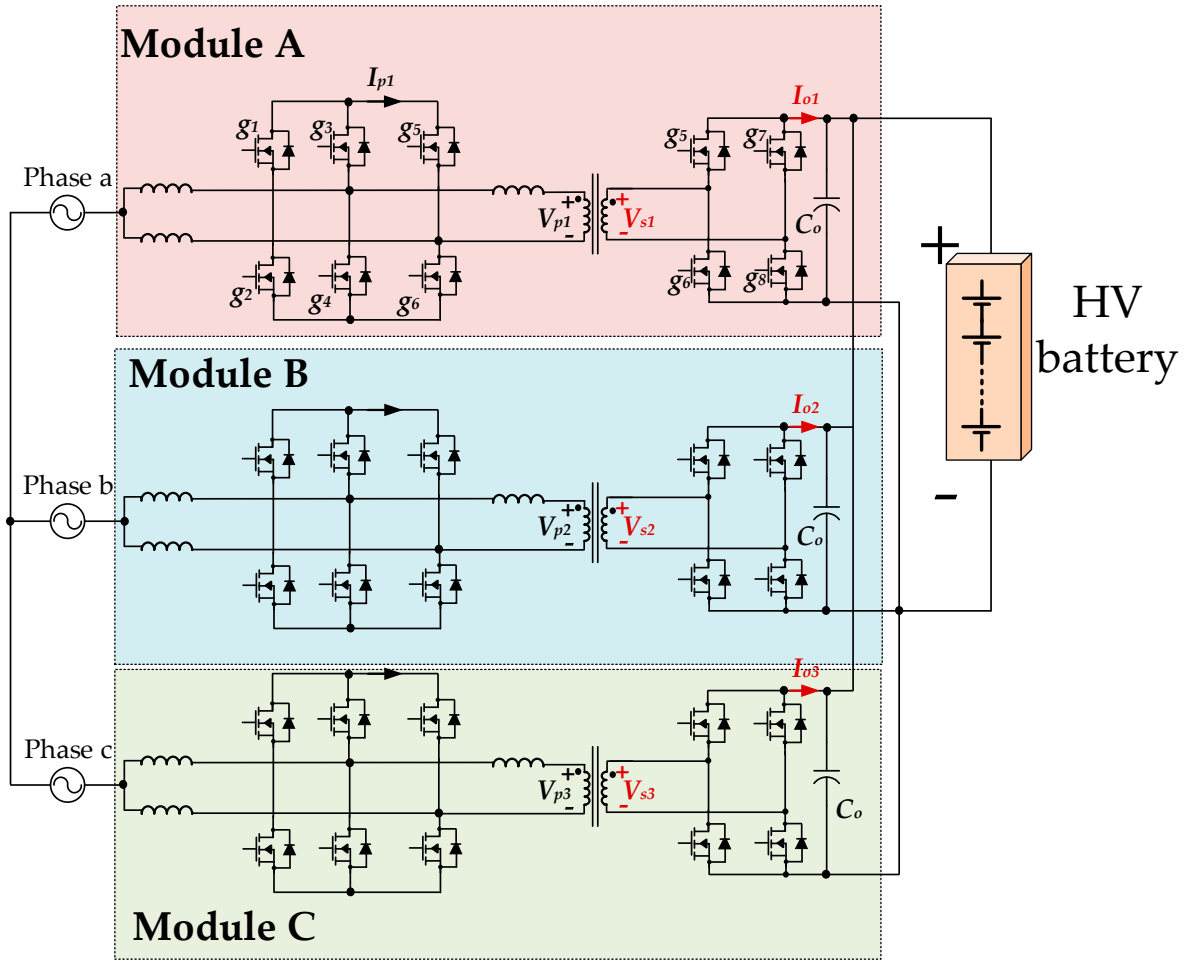

Figure 27. The single-stage three-phase OBC in [52].

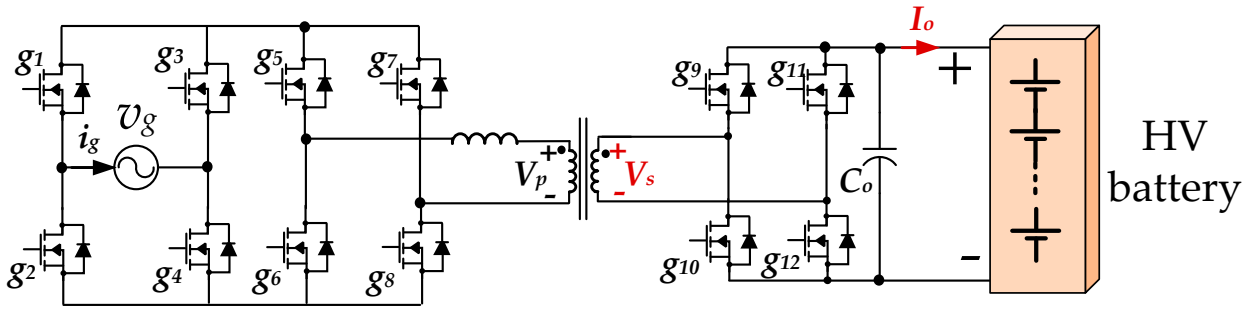

Figure 28. The single-phase OBC in [54].

Table 5. Summary of the reviewed EV modular charging systems.

Refs.	Topology	Power	Grid	Switching Freq.	Year	Remarks
[40]	MMC/FB	—	MVAC	—	2021	High circulating current during unbalanced charging
[41]	MMC/FB	—	MVAC	—	2021	Control system to solve arm current imbalance
[42]	MAB	—	MVAC	50 kHz	2024	The input rectifier is not modular
[44]	MMC/FB	320 kW	MVDC	400 Hz	2023	Complicated MFMT design
[48]	VSI/VDS	320 kW	LVAC	16 kHz	2019	Circulating currents need consideration
[49]	DAB	75 kW	MVAC	20 kHz	2022	High-output DC voltage
[51]	DAB	22 kW	LVAC	5 kHz	2014	Unidirectional power flow; no V2G capability
[52]	DAB	7.4 kW	LVAC	150 kHz	2021	Three-phase bidirectional power
[54]	DAB	600 W	LVAC	25 kHz	2018	Single-phase/bidirectional power

5. Cascaded Modular Machines

Traction electrical machines are a critical element in EVs that determine efficiency; therefore, they are required to have high torque, power density, and reliability [55]. The machines are also required to provide this high efficiency and torque over the majority of the speed range [56]. Although conventional machines such as PMSM and IM can provide good efficiency at medium speeds, they suffer from lowered efficiency at low and high speeds as well as an inability to fault ride-through [57]. Thus, extensive research efforts have attempted to explore multi-phase machines and multi-machine systems to enhance the machine's performance and reliability [58,59].

Modular cascaded machines (MCMs) have been proposed, in which conventional machines are still used but with a different connection architecture. For example, multiple machines can be connected end-to-end through shafts to make their torque independent while having the same rotational speeds. Also, multiple machines can be connected in parallel with specially designed gears and mechanical couplings, so they have different torques and speeds. The main goals of MCM architectures are to improve the propulsion system characteristics by increasing the available power and torque, extend system efficiency by adjusting the number and the connection of the modular machines, and improve propulsion system reliability when a machine breaks down [60]. Also, as diverse types of electrical machines have their own merits and advantages; combining more than one type in the same EV propulsion system can improve performance when benefiting from the advantages of each type. The provided flexibility, additional degrees of freedom, and increased controllability add to the modular system's complexity in comparison with the single electric drive system; therefore, smart energy management systems (EMSs) will be required.

In [61], an interior permanent magnet machine (IPM) and PM-assisted synchronous reluctance motor (PMa-SynRM) are integrated to take advantage of each machine type. The PMa-SynRM is a recent technology that can achieve high efficiency over a wide speed range without using rare earth magnets; therefore, it is viewed as a candidate to replace PMSMs [61]. The combination of IPM and PMa-SynRM in the EV traction system, as shown in Figure 29, aims to improve performance, increase energy efficiency, and reduce cost. Three configurations were compared including (1) a rear-wheel drive train with an IPM, single-battery, and a mechanical differential; (2) all-wheel drive (AWD) with an IPM at the front shaft and a PMa-SynRM at the rear shaft; and (3) AWD with a combination of IPM and PMa-SynRM with individual batteries and inverters.

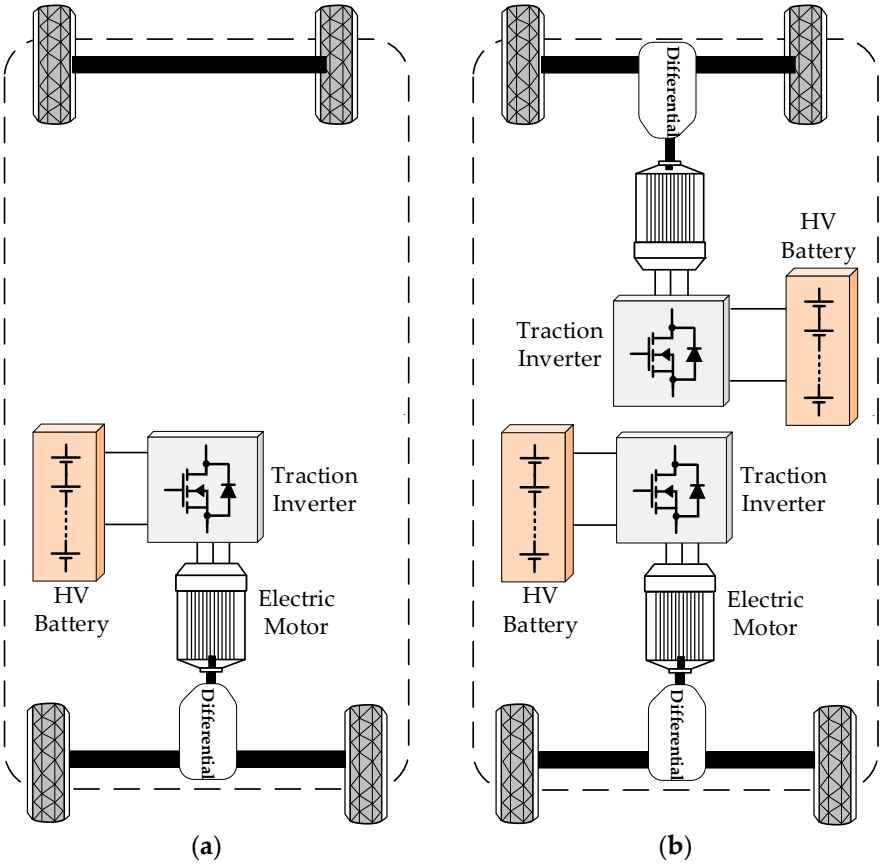

Figure 29. MCM drivetrain configurations: (**a**) rear-wheel drive and (**b**) all-wheel drive with different motors [61].

The simulation results reveal that the third configuration is able to improve efficiency by more than 2% with a further improvement in energy harvesting using flexible control strategies. The authors suggest that using PMa-SynRM at the front shaft and using the IPM at the rear shaft improves energy efficiency as the former has high efficiency at high speed while the latter provides its best efficiency at medium and low speeds. On the downside, the AWD configuration with two different motors leads to an increase in total system weight by a few kilograms.

In [62], PMSM and IM are combined in series on the same main shaft, which is connected to the back wheels through a reduction gearbox, as shown in Figure 30. Each motor has an individual DC/AC inverter supplied by a common HV battery. The experiments show a 5% saving in the delivered energy to the motors. The optimal machine sizes are selected and simulated using the finite element method (FEM), and the results suggest that 53% of the permanent magnet usage can be saved in comparison with a single PMSM. However, the paper did not test the real-time operation of the proposed MCM system in

normal driving and braking, and it may be necessary to explore the hybrid motor combination effect on the EV total torque and speed and hence, on the traction inverters and battery systems.

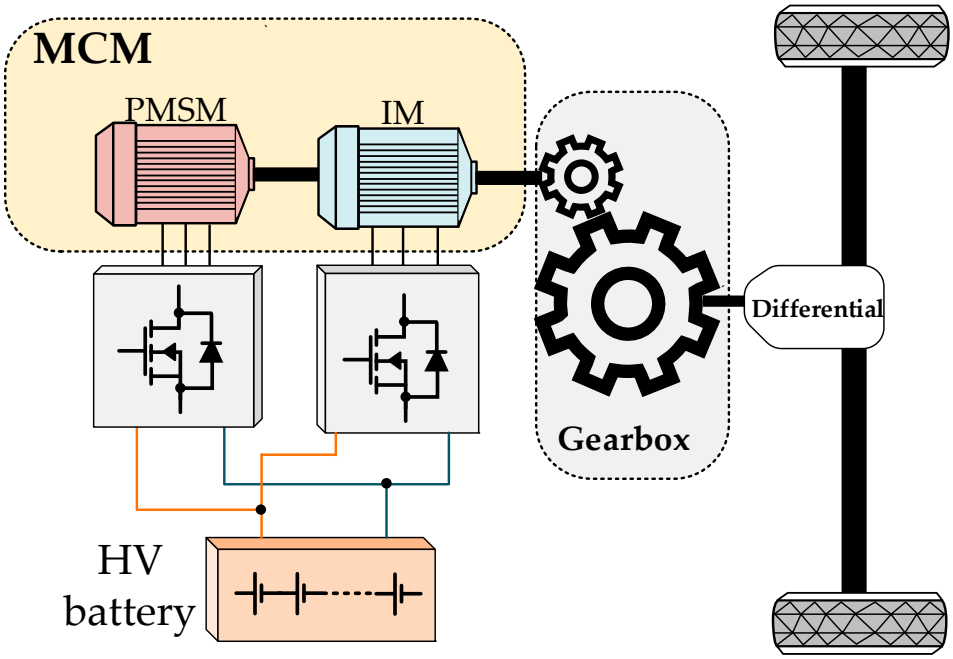

Figure 30. The hybrid MCM with PMSM and IM in [62].

The idea of cascading machines at different power levels is explored in [63]. The system in Figure 31 shows the EV propulsion system configuration when two electric machines at 14 kW and 21 kW are connected in series to the rear wheel shaft. Accordingly, the two machines have the same speeds, but their torques can be independent. The EV total torque is the summation of the two motor torques. The study is carried out with different driving cycles and reveals that the propulsion system based on the MCM configuration consumes less energy than the single-drive EV at the same total power, which is 35 kW. The authors estimate the system energy saving to be in the range of 6% to 10%, which can have a significant impact on battery size and the cooling system.

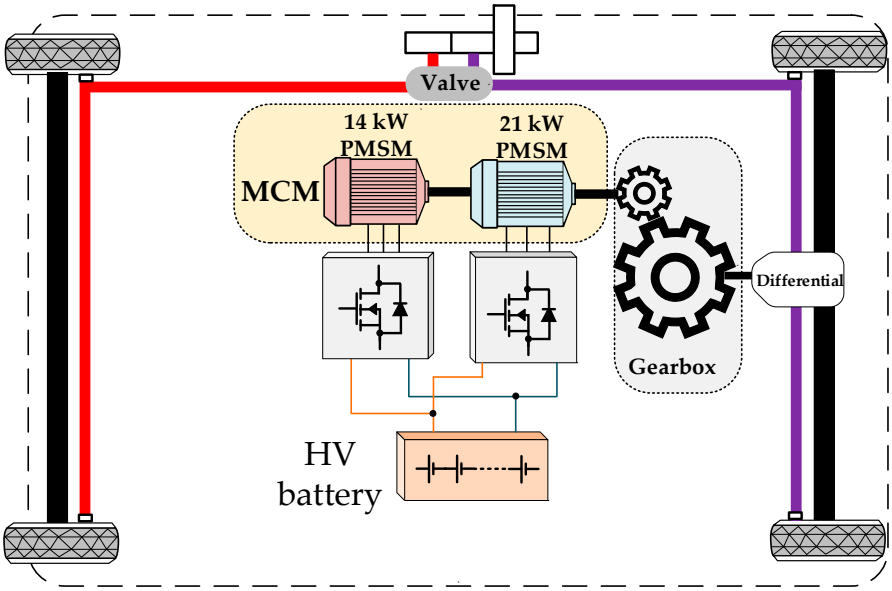

Figure 31. Hybrid MCM with PSMSs of different power ratings [63].

6. Discussion

The modular electrical structures in the literature can provide the required scalability for promoting the GMP, which can support the EV sector in different ways. Modular EV battery systems increase the degree of flexibility in the design process for different sizes and power ratings and allow for employing different battery technologies and electrochemical materials. Modular propulsion systems can split the dc-link voltage of the motor from the battery module voltages and hence, decouple motor performance and its traction inverter from the battery system. Modular chargers can provide scalability and redundancy for the EV sector as power module units can be employed for different EV sizes as well as the charging infrastructure itself. Similarly, MCM systems can support the GMP concept by increasing the level of scalability, redundancy, and fault tolerance of EVs during the design process and operation. In general, modularising EV electrical systems can reduce semiconductor device voltage and current stresses in the modular units. This facilitates employing wide-bandgap (WBG) semiconductor devices that can reduce power losses and size dramatically.

According to the conducted review in the previous sections, the following points can be observed:

- Although computer simulations showed that the efficiency of the single-stage CHB-based modular EV system [29] is higher than the converters in [30,32], as shown in Figure 8, it has lower controllability as it is difficult to control the input and output simultaneously.
- Although the efficiency of the SEPIC-based converter in [32] is lower than the CHB-based converter in [29], the former has continuous constant current, as shown in Figure 7c, which is favoured for extending battery cell lifetime. Also, the SEPIC modules allow for galvanic isolation, which is necessary for complying with grid standards.
- The numerical findings are obtained from computer simulations at a specific number of SMs (four in this case); therefore, further studies are needed to explore and compare the performances of modular EV systems when the number of SMs is varied.
- A visual representation of a comparison among modular EV battery systems is shown in the spider-web diagram in Figure 32.

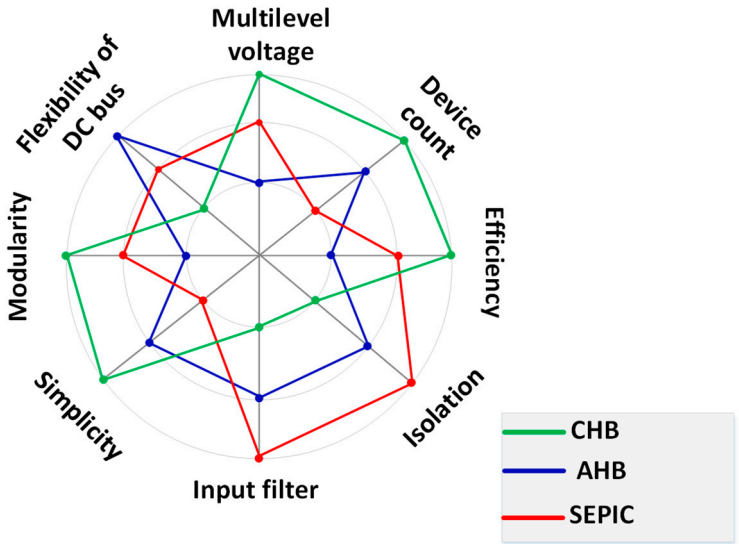

Figure 32. Comparison of the reviewed modular EV battery systems (green: [29], blue: [30], and red: [32]).

- Based on the efficiency comparison for modular traction inverters in Figure 18, the asymmetrical CHB inverter efficiency in [34] is the lowest when compared with the CHB inverter in [33] and the T-type inverter in [38]. However, this is affected by the

losses in the auxiliary stage's semiconductor devices as well as the isolation HFTs that are missing from the other two systems.

- Thanks to the additional auxiliary stage, the asymmetrical CHB in [34] has the lowest torque ripple compared with the other two systems.
- The efficiency comparisons in Figure 18 are not necessarily the same if the systems are extended and tested under variable power levels and SM numbers.
- A visual representation comparing modular EV traction inverters is shown in the spider-web diagram in Figure 33.

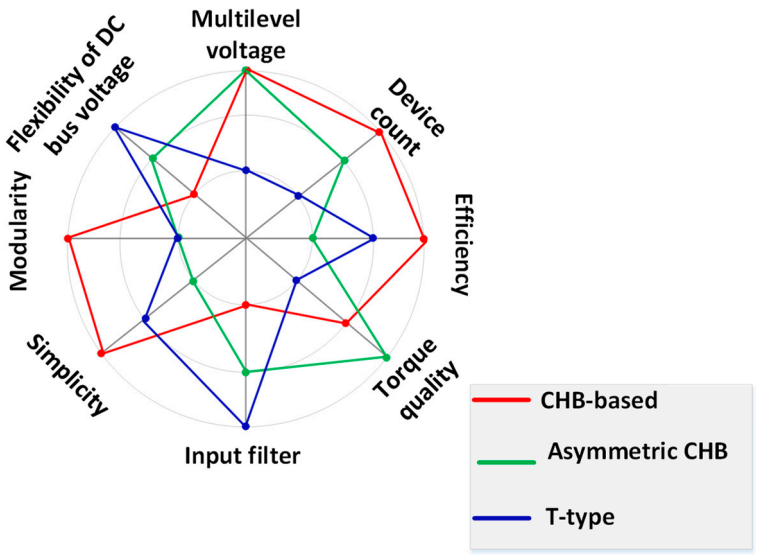

Figure 33. Comparison of the reviewed modular EV traction inverters (red: [33], green: [34], and blue: [38]).

- Because of its simple construction and control system, the DAB converter dominates the publications on modular charging systems, and there is a gap in exploring other isolated power converters that can be alternatives to reduce HFT size and provide better THD for input and output currents.
- The work conducted on MCM systems is limited to two research groups, and more research effort needs to be conducted in this area so the modularisation of the EV electric systems can progress at the same level.

7. Conclusions

This paper explored the attractiveness of modular power converters and machine structures in the context of EVs by providing an overview of the research literature. Several EV manufacturers, including Volkswagen, GE, Tesla, and Hyundai are exploring the feasibility of modular platform concepts in the future of the EV sector. The modular platform provides EV manufacturers with more flexibility in designing and testing several combinations of motors, chargers, power converters, and drives.

Starting from the battery system, this paper reviewed the main modular topologies that can be useful in splitting an HV battery into smaller and lighter segments. A modular battery system can add several advantages to the EV system such as better controllability, energy management, and a flexible dc-link. However, this comes at the expense of more complicated control, wiring, and communication. The CHB is the most common power electronic topology in modular battery systems because of its cascaded connection. Modular traction inverters can add a significant improvement to the performance of tractive systems during normal driving and faulty conditions. However, the modular inverter power density needs to be improved significantly to be able to compete with conventional systems. Battery chargers, whether OBCs or DC fast chargers, can benefit from the increased possible power limits provided by modular structures with several units that can deliver higher

charging currents to battery segments. Inspired by the recent advancement in modular HVDC systems, most of the publications on modular EV chargers focused on modularising the DC/DC converters in battery chargers while a few considered an AC/DC rectifier stage. Examining publications on cascaded modular machine systems combining different machine types such as PMSM, IMs, and PM-SynRA can provide advantages to EVs in terms of increased torque, reduced size, and less dependability on rare earth magnetic materials.

Author Contributions: Conceptualisation, A.D. and M.A.E.; analysis, A.D.; methodology, A.D., M.A.E. and B.W.W.; software, A.D.; writing—review and editing, A.D., M.A.E. and B.W.W. All authors have read and agreed to the published version of the manuscript.

Funding: This research received no external funding.

Conflicts of Interest: The authors declare no conflicts of interest.

References

1. Li, Z.; Khajepour, A.; Song, J. A comprehensive review of the key technologies for pure electric vehicles. *Energy* **2019**, *182*, 824–839. [CrossRef]
2. Sun, X.; Li, Z.; Wang, X.; Li, C. Technology development of electric vehicles: A review. *Energies* **2020**, *1*, 90. [CrossRef]
3. Cai, W.; Wu, X.; Zhou, M.; Liang, Y.; Wang, Y. Review and Development of Electric Motor Systems and Electric Powertrains for New Energy Vehicles. *Automot. Innov.* **2021**, *4*, 3–22. [CrossRef]
4. Nasr Esfahani, F.; Darwish, A.; Williams, B.W. Power Converter Topologies for Grid-Tied Solar Photovoltaic (PV) Powered Electric Vehicles (EVs)—A Comprehensive Review. *Energies* **2022**, *15*, 4648. [CrossRef]
5. Mills, M.; Obi, M.; Cody, K.; Garton, K.; Wisser, A.M.; Nabahani, S. Utility Planning for Distribution-Optimized Electric Vehicle Charging: A Case Study in the United States Pacific Northwest. *IEEE Power Energy Mag.* **2023**, *21*, 48–55. [CrossRef]
6. Nasr Esfahani, F.; Darwish, A.; Ma, X.; Twigg, P. Non-Integrated and Integrated On-Board Battery Chargers (iOBCs) for Electric Vehicles (EVs): A Critical Review. *Energies* **2024**, *17*, 2285. [CrossRef]
7. Stippich, A.; Van Der Broeck, C.H.; Sewergin, A.; Wienhausen, A.H.; Neubert, M.; Schülting, P.; Taraborrelli, S.; van Hoek, H.; De Doncker, R.W. Key components of modular propulsion systems for next generation electric vehicles. *CPSS Trans. Power Electron. Appl.* **2017**, *2*, 249–258. [CrossRef]
8. Schulz, S.E. Exploring the high-power inverter: Reviewing critical design elements for electric vehicle applications. *IEEE Electrif. Mag.* **2017**, *5*, 28–35. [CrossRef]
9. Rajashekara, K. Present status and future trends in electric vehicle propulsion technologies. *IEEE J. Emerg. Sel. Top. Power Electron.* **2013**, *1*, 3–10. [CrossRef]
10. Lee, H.K.; Nam, K.H. An Overview: Current Control Technique for Propulsion Motor for EV. *Trans. Korean Inst. Power Electron.* **2016**, *21*, 388–395. [CrossRef]
11. Meddour, A.R.; Rizoug, N.; Leserf, P.; Vagg, C.; Burke, R.; Larouci, C. Optimization of the Lifetime and Cost of a PMSM in an Electric Vehicle Drive Train. *Energies* **2023**, *16*, 5200. [CrossRef]
12. Park, K.; Jung, S.; Kim, S.; Ko, J. Generated Voltage Control of EV PMSM for Maximizing Energy Recovery Rate using Switched Resonant L-C. In Proceedings of the 2019 14th Annual Conference System of Systems Engineering (SoSE), Anchorage, AK, USA, 19–22 May 2019; pp. 195–199.
13. Antony, R.P.; Komarasamy, P.R.G.; Rajamanickam, N.; Alroobaea, R.; Aboelmagd, Y. Optimal Rotor Design and Analysis of Energy-Efficient Brushless DC Motor-Driven Centrifugal Monoset Pump for Agriculture Applications. *Energies* **2024**, *17*, 2280. [CrossRef]
14. El Hadraoui, H.; Zegrari, M.; Chebak, A.; Laayati, O.; Guennouni, N. A Multi-Criteria Analysis and Trends of Electric Motors for Electric Vehicles. *World Electr. Veh. J.* **2022**, *13*, 65. [CrossRef]
15. Monteiro, J.R.; Oliveira, A.A.; Aguiar, M.L.; Sanagiotti, E.R. Electromagnetic torque ripple and copper losses reduction in permanent magnet synchronous machines. *Eur. Trans. Electr. Power* **2012**, *22*, 627–644. [CrossRef]
16. Jing, L.B.; Cheng, J. Research on torque ripple optimization of switched reluctance motor based on finite element method. *Prog. Electromagn. Res.* **2018**, *74*, 115–123. [CrossRef]
17. Shin, S.; Kawagoe, N.; Kosaka, T.; Matsui, N. Study on commutation control method for reducing noise and vibration in SRM. *IEEE Trans. Ind. Appl.* **2018**, *54*, 4415–4424. [CrossRef]
18. Larminie, J.; Lowry, J. Electric Machines and their Controllers. In *Electric Vehicle Technology Explained*, 2nd ed.; Wiley: Hoboken, NJ, USA, 2012; Chapter 6; pp. 141–181.
19. Buddyelectric. The Electric Car from Norway Made by ElBil Norge. Available online: https://www.kewet.de/downloads/kewetbuddyprospekt2.pdf (accessed on 1 June 2024).
20. Nasr Esfahani, F.; Darwish, A.; Massoud, A. PV/Battery Grid Integration Using a Modular Multilevel Isolated SEPIC-Based Converter. *Energies* **2022**, *15*, 5462. [CrossRef]

21. Xu, Z.; Li, T.; Zhang, F.; Zhang, Y.; Lee, D.-H.; Ahn, J.-W. A Review on Segmented Switched Reluctance Motors. *Energies* **2022**, *15*, 9212. [CrossRef]
22. Hyundai Newsroom. The Pump-to-Plug Revolution. Available online: https://www.hyundai.com/worldwide/en/brand-journal/ioniq/e-gmp-revolution (accessed on 1 June 2024).
23. Kia Press-Releases. Hyundai Motor Group to Lead Charge into Electric Era with Dedicated EV Platform. Available online: https://press.kia.com/eu/en/home/media-resouces/press-releases/2020/EV_Platform_E_GMP.html (accessed on 1 June 2024).
24. Volkswagen Newsroom. Modular Electric Drive Matrix. Available online: https://www.volkswagen-newsroom.com/en/modular-electric-drive-matrix-meb-3677 (accessed on 1 June 2024).
25. Darwish, A.; Holliday, D.; Finney, S. Operation and control design of an input series–input-parallel–output-series conversion cheme for offshore DC wind systems. *IET Power Electron.* **2017**, *10*, 2092–2103. [CrossRef]
26. Rabiul Islam, M.; Mahfuz-Ur-Rahman, A.M.; Muttaqi, K.M.; Sutanto, D. State-of-the-Art of the Medium-Voltage Power Converter Technologies for Grid Integration of Solar Photovoltaic Power Plants. *IEEE Trans. Energy Convers.* **2019**, *34*, 372–384. [CrossRef]
27. Alotaibi, S.; Darwish, A.; Williams, B.W. Three-phase inverter based on isolated SEPIC/CUK converters for large-scale PV applications. *Int. J. Electr. Power Energy Syst.* **2023**, *146*, 108723. [CrossRef]
28. Tolbert, L.; Peng, F.Z.; Cunnyngham, T.; Chiasson, J. Charge balance control schemes for cascade multilevel converter in hybrid electric vehicles. *IEEE Trans. Ind. Electron.* **2002**, *49*, 1058–1064. [CrossRef]
29. Evzelman, M.; Rehman, M.M.; Hathaway, K.; Zane, R.; Costinett, D.; Maksimovic, D. Active balancing system for electric vehicles with incorporated low-voltage bus. *IEEE Trans. Power Electron.* **2016**, *31*, 7887–7895. [CrossRef]
30. Gan, C.; Sun, Q.; Wu, J.; Kong, W.; Shi, C.; Hu, Y. MMC-Based SRM Drives with Decentralized Battery Energy Storage System for Hybrid Electric Vehicles. *IEEE Trans. Power Electron.* **2019**, *34*, 2608–2621. [CrossRef]
31. Theliander, O.; Kersten, A.; Kuder, M.; Han, W.; Grunditz, E.A.; Thiringer, T. Battery Modeling and Parameter Extraction for Drive Cycle Loss Evaluation of a Modular Battery System for Vehicles Based on a Cascaded H-Bridge Multilevel Inverter. *IEEE Trans. Ind. Appl.* **2020**, *56*, 6968–6977. [CrossRef]
32. Nasr Esfahani, F.; Darwish, A.; Ma, X. Design and Control of a Modular Integrated On-Board Battery Charger for EV Applications with Cell Balancing. *Batteries* **2024**, *10*, 17. [CrossRef]
33. Du, Z.; Ozpineci, B.; Tolbert, L.M.; Chiasson, J.N. DC–AC Cascaded H-Bridge Multilevel Boost Inverter with No Inductors for Electric/Hybrid Electric Vehicle Applications. *IEEE Trans. Ind. Appl.* **2009**, *45*, 963–970. [CrossRef]
34. Pereda, J.; Dixon, J. 23-Level Inverter for Electric Vehicles Using a Single Battery Pack and Series Active Filters. *IEEE Trans. Veh. Technol.* **2012**, *61*, 1043–1051. [CrossRef]
35. Sun, Q.; Wu, J.; Gan, C.; Si, J.; Guo, J.; Hu, Y. Cascaded Multiport Converter for SRM-Based Hybrid Electrical Vehicle Applications. *IEEE Trans. Power Electron.* **2019**, *34*, 11940–11951. [CrossRef]
36. Zhang, Y.; Chen, G.; Hu, Y.; Gong, C.; Wang, Y. Cascaded multilevel inverter based power and signal multiplex transmission for electric vehicles. *CES Trans. Electr. Mach. Syst.* **2020**, *4*, 123–129. [CrossRef]
37. Badawy, M.O.; Sharma, M.; Hernandez, C.; Elrayyah, A.; Guerra, S.; Coe, J. Model Predictive Control for Multi-Port Modular Multilevel Converters in Electric Vehicles Enabling HESDs. *IEEE Trans. Energy Convers.* **2022**, *37*, 10–23. [CrossRef]
38. Sheir, A.; Youssef, M.Z.; Orabi, M. A Novel Bidirectional T-Type Multilevel Inverter for Electric Vehicle Applications. *IEEE Trans. Power Electron.* **2019**, *34*, 6648–6658. [CrossRef]
39. Rathore, V.; Rajashekara, K.; Nayak, P.; Ray, A. A High-Gain Multilevel Dc–Dc Converter for Interfacing Electric Vehicle Battery and Inverter. *IEEE Trans. Ind. Appl.* **2022**, *58*, 6506–6518. [CrossRef]
40. Aditya, K.; Pradhan, S.; Munsi, A. Feasibility study on megawatt-level fast charging system for shore power supply using wireless power transfer technology. *Electr. Eng.* **2024**, *108*, 1569–1583. [CrossRef]
41. Guidi, G.; D'Arco, S.; Nishikawa, K.; Suul, J.A. Load Balancing of a Modular Multilevel Grid-Interface Converter for Transformer-Less Large-Scale Wireless Electric Vehicle Charging Infrastructure. *IEEE J. Emerg. Sel. Top. Power Electron.* **2021**, *9*, 4587–4605. [CrossRef]
42. Cai, Y.; Li, J.; Gu, C.; Yang, J.; Guenter, S.; Buticchi, G.; Zhang, H. A Modular Modulation Decoupling Algorithm for Multiple Active Bridge Based Multiport EV Charger. *IEEE J. Emerg. Sel. Top. Power Electron.* **2024**. *Early access*. [CrossRef]
43. Darwish, A.; Wang, Y.; Holliday, D.; Finney, S. Operation and control design of new Three-Phase inverters with reduced number of switches. In Proceedings of the International Symposium on Power Electronics, Electrical Drives, Automation and Motion (SPEEDAM), Capri, Italy, 22–24 June 2016; pp. 178–183.
44. Sarkar, S.; Das, A. An Isolated Single Input-Multiple Output DC–DC Modular Multilevel Converter for Fast Electric Vehicle Charging. *IEEE J. Emerg. Sel. Top. Ind. Electron.* **2023**, *4*, 178–187. [CrossRef]
45. Celli, G.; Soma, G.G.; Pilo, F.; Lacu, F.; Mocci, S.; Natale, N. Aggregated electric vehicles load profiles with fast charging stations. In Proceedings of the 2014 Power Systems Computation Conference, Wroclaw, Poland, 18–22 August 2014; pp. 1–7.
46. Scirè, D.; Lullo, G.; Vitale, G. Design and Modeling of an Interleaving Boost Converter with Quasi-Saturated Inductors for Electric Vehicles. In Proceedings of the 2020 AEIT International Conference of Electrical and Electronic Technologies for Automotive (AEIT AUTOMOTIVE), Turin, Italy, 18–20 November 2020; pp. 1–6. [CrossRef]
47. Sferlazza, A.; Garraffa, G.; Vitale, G.; D'Ippolito, F.; Alonge, F.; Lullo, G.; Busacca, A.; Giaconia, G.C.; Scirè, D. Robust Disturbance Rejection Control of DC/DC Interleaved Boost Converters with Additional Sliding Mode Component. In Proceedings of the 2023 Asia Meeting on Environment and Electrical Engineering (EEE-AM), Hanoi, Vietnam, 13–15 November 2023; pp. 1–6. [CrossRef]

48. Drobnic, K.; Grandi, G.; Hammami, M.; Mandrioli, R.; Ricco, M.; Viatkin, A.; Vujacic, M. An Output Ripple-Free Fast Charger for Electric Vehicles Based on Grid-Tied Modular Three-Phase Interleaved Converters. *IEEE Trans. Ind. Appl.* **2019**, *55*, 6102–6114. [CrossRef]
49. Lam, H.S.; Yuan, H.; Tan, S.-C.; Mi, C.C.; Pou, J.; Hui, S.Y.R. Bidirectional AC–DC Modular Multilevel Converter With Electric Spring Functions for Stabilizing Renewable AC Power Grid at the Distribution Voltage Level. *IEEE J. Emerg. Sel. Top. Power Electron.* **2022**, *10*, 7589–7600. [CrossRef]
50. Khaligh, A.; D'Antonio, M. Global trends in high-power on-board chargers for electric vehicles. *IEEE Trans. Veh. Technol.* **2019**, *68*, 3306–3324. [CrossRef]
51. Schmenger, J.; Endres, S.; Zeltner, S.; Marz, M. A 22 kW on-board charger for automotive applications based on a modular design. In Proceedings of the 2014 IEEE Conference on Energy Conversion (CENCON), Bahru, Malaysia, 13–14 October 2014; pp. 1–6.
52. Kim, H.; Park, J.; Kim, S.; Hakim, R.M.; Kieu, H.P.; Choi, S. Single-Stage EV On-Board Charger with Single- and Three-Phase Grid Compatibility. In Proceedings of the 2021 IEEE Applied Power Electronics Conference and Exposition (APEC), Phoenix, AZ, USA, 14–17 June 2021; pp. 583–589.
53. Wouters, H.; Martinez, W. Bidirectional On-Board Chargers for Electric Vehicles: State-of-the-Art and Future Trends. *IEEE Trans. Power Electron.* **2023**, *39*, 693–716. [CrossRef]
54. Kisacikoglu, M.C. A Modular Single-Phase Bidirectional EV Charger with Current Sharing Optimization. In Proceedings of the 2018 IEEE Transportation Electrification Conference and Expo (ITEC), Long Beach, CA, USA, 13–15 June 2018; pp. 366–371. [CrossRef]
55. Diallo, D.; Benbouzid, M.E.H.; Makouf, A. A fault-tolerant control architecture for induction motor drives in automotive applications. *IEEE Trans. Veh. Techn.* **2004**, *53*, 1847–1855. [CrossRef]
56. Diallo, D.; Benbouzid, M.E.H.; Masrur, M.A. Special Section on Condition Monitoring and Fault Accommodation in Electric and Hybrid Propulsion Systems. *IEEE Trans. Veh. Technol.* **2013**, *62*, 962–964. [CrossRef]
57. Liu, G.; Yang, J.; Zhao, W.; Ji, J.; Chen, Q.; Gong, W. Design and analysis of a new fault-tolerant permanent magnet vernier machine for electrical vehicles. *IEEE Trans. Magn.* **2012**, *48*, 4176–4179. [CrossRef]
58. Hua, W.; Yin, X.M.; Zhang, G.; Cheng, M. Analysis of Two Novel Five-Phase Hybrid-Excitation Flux-Switching Machines for Electric Vehicles. *IEEE Trans. Magn.* **2014**, *50*, 8700305. [CrossRef]
59. Yuan, X.; Wang, J. Torque distribution strategy for a front-and rear-wheel-driven electric vehicle. *IEEE Trans. Veh. Technol.* **2012**, *61*, 3365–3374. [CrossRef]
60. Li, K.; Han, S.; Cui, S.; Bouscayrol, A. Sizing of modular cascade machines system for electric vehicles. *IEEE Trans. Veh. Technol.* **2019**, *68*, 1278–1287. [CrossRef]
61. Huynh, T.-A.; Chen, P.-H.; Hsieh, M.-F. Analysis and Comparison of Operational Characteristics of EV Traction Units Combining Two Different Types of Motors. *IEEE Trans. Veh. Technol.* **2022**, *71*, 5727–5742. [CrossRef]
62. Li, K.; Bouscayrol, A.; Cui, S.; Cheng, Y. A Hybrid Modular Cascade Machines System for Electric Vehicles Using Induction Machine and Permanent Magnet Synchronous Machine. *IEEE Trans. Veh. Technol.* **2020**, *70*, 273–281. [CrossRef]
63. Li, K.B.; Bouscayrol, A.; Han, S.L.; Cui, S.M. Comparisons of Electric Vehicles Using Modular Cascade Machines System and Classical Single Drive Electric Machine. *IEEE Trans. Veh. Technol.* **2018**, *67*, 354–361. [CrossRef]